2012-01-01

Further Characterization Of The Nodamura Virus Rna2 3'-Terminal Stem Loop Structure And Its Role In Viral Rna Replication

Joshua Frederick
University of Texas at El Paso, jpfrederick@miners.utep.edu

FURTHER CHARACTERIZATION OF THE *NODAMURA VIRUS* RNA2

3'-TERMINAL STEM LOOP STRUCTURE AND ITS ROLE IN

VIRAL RNA REPLICATION

JOSHUA P. FREDERICK

Department of Biological Sciences

APPROVED:

_____

Kyle L. Johnson, Ph.D., Chair

_____

Manuel Llano, M.D., Ph.D.

_____

Germán Rosas-Acosta, Ph.D.

_____

Chuan Xiao, Ph.D.

_____

Benjamin C. Flores, Ph.D.
Dean of the Graduate School

FURTHER CHARACTERIZATION OF THE *NODAMURA VIRUS* RNA2 3'-TERMINAL STEM LOOP STRUCTURE AND ITS ROLE IN VIRAL RNA REPLICATION

By

JOSHUA P. FREDERICK, B.S.

THESIS

Presented to the Faculty of the Graduate School of

The University of Texas at El Paso

in Partial Fulfillment

of the Requirements

for the Degree of

MASTER OF SCIENCE

Department of Biological Sciences

THE UNIVERSITY OF TEXAS AT EL PASO

December 2012

ACKNOWLEDGEMENTS

I would like to thank the following persons for their aid in the completion of this work:

Dr. Kyle L. Johnson
For her mentorship, guidance and the experience provided in her laboratory, as well as financial support. Thank you Dr. J! I have learned and grown so much under your wing. Thank you from the bottom of my heart.

Dr. Manuel Llano
Dr. Germán Rosas-Acosta
Dr. Chuan Xiao
For their support as committee members

Dr. Ming-Ying Leung
For financial support

Vincent U. Gant Jr.
For many helpful conversations and troubleshooting advice. I couldn't have done it without you! I wish you the best of luck in all of your endeavors, Vince!

Ana Betancourt
For DNA sequencing services, as well as construction of plasmids pT7RNoV2-S1comp, pT7RNoV2-S2comp, pT7RNoV2-S1S2 (Dbl), pT7RNoV2-S1neg, and pT7RNoV2-S2pos, and pT7RNoV2-Δ656

Dana C. Galvan
For assistance in reconstruction and testing of plasmid pT7RNoV2-Δ655

Karla M. Viramontes
For experimental assistance and analysis of several NoV2 derivatives, especially NoV2-Δ3'10

Lani Alcazar
For assistance in using equipment provided by the Border Biomedical Research Center Biomolecule Analysis Core Facility

The past and present members of the Johnson laboratory

Lee H. Frederick and Janet G. Frederick
For their abundant love and support. I love you both very much!

TABLE OF CONTENTS

Page

LIST OF TABLES

Page

LIST OF FIGURES

Table 1: Thermodynamic properties of NoV RNA2 derivatives under investigation.

	Oligomer		Full-Length RNA2	
RNA2	**ΔG (kcal/mol)**	**ΔΔG (kcal/mol)**	**ΔG (kcal/mol)**	**ΔΔG (kcal/mol)**
WT	-8.40	--	-453.40	--
ΔSL	--	--	-443.50	9.90
S1neg	-4.20	4.20	-447.80	5.60
S2pos	2.90	11.30	-444.00	9.40
Up	-4.40	4.00	-455.10	-1.70
Down	2.50	10.90	-445.40	8.00
Dbl	-7.90	0.50	-452.30	1.10
S1T	-4.60	3.80	-454.20	-0.80
S2T	0.10	8.50	-446.10	7.30
DST	-7.20	1.20	-450.40	3.00
ΔSBP	-0.50	7.90	-444.40	9.00
TransLoop	-9.20	-0.80	-454.20	-0.80
4Loop	-11.60	-3.20	-455.10	-1.70
3Loop	-8.90	-0.50	-453.40	0.00
ΔLoop	-6.70	1.70	-452.30	1.10
Δ656	--	--	-447.20	6.20
Δ655	--	--	-447.20	6.20
655T	--	--	-448.20	5.20
MLRI	--	--	-449.00	4.40

All data generated using the mfold web server (Zuker, 2003).

ABBREVIATIONS USED IN THIS STUDY

ANOVA – analysis of variance
ATP – adenosine triphosphate
BBV – *Black beetle virus*
BoV – *Boolarra virus*
cDNA – complementary DNA
DNA – deoxyribonucleic acid
FHV – *Flock house virus*
GGNNV – *Greasy grouper nervous necrosis virus*
gRNA – genomic RNA
HDV Rz – *Hepatitis delta virus* antigenomic ribozyme
LRI – long range interaction
NoV- *Nodamura virus*
ORF – open reading frame
PAP – polyadenosine polymerase; poly(a) polymerase
PCR – polymerase chain reaction
RBP – RNA-binding protein
RdRp – RNA dependent RNA polymerase
RNA – ribonucleic acid
sgCE – subgenomic control element
sgRNA – subgenomic RNA
SJNNV – *Striped jack nervous necrosis virus*
SL – stem loop
TLS – tRNA-like structure
UTR – untranslated region
vRNA – viral RNA
WhNV – *Wuhan nodavirus*
WT – wildtype

CHAPTER 1

PURPOSE AND SIGNIFICANCE

Nodamura virus (NoV) is an excellent model system for studying many aspects of the life cycle of positive-strand RNA viruses. NoV's simple genome organization and ability to replicate its genome to high levels in a wide variety of host cells, including plants, yeast, insects and mammals (Ball et al., 1992; Garzon et al., 1978, 1990; Murphy et al., 1970; Price et al., 2005; Scherer & Hurlbut, 1967; Selling et al., 1990; reviewed by Ball & Johnson, 1998), make it a prime model system for studying the basic mechanisms of viral RNA replication. Other positive-strand RNA viruses, including those that are pathogenic for humans, may share these mechanisms. Additionally, these studies together suggest that the host factors involved in NoV RNA replication must be widely conserved across many eukaryotic organisms. NoV is unique in its lethality for both invertebrates and mammals, as other nodaviruses are nonpathogenic for higher vertebrates (Bailey et al., 1975; Longworth & Carey, 1976; Ball & Johnson, 1998) and cannot replicate at 37^{o}C (Ball et al., 1992). These characteristics support the idea of NoV serving as a simplified model system for more complex positive-strand RNA human pathogens, particularly arboviruses and picornaviruses. In defining the minimum essential *cis*-acting elements required for nodavirus RNA replication, previous work in our laboratory predicted the presence of a conserved stem-loop structure in the 3' untranslated region (UTR) of NoV RNA2, verified its existence biochemically, and showed that it that acts as a *cis*-acting replication element in chimeric NoV RNA2-based replicons in transformed yeast cells (Rosskopf et al., 2010; Taufer et al., 2008). RNA

structures in the 3' UTRs of viral RNAs represent ubiquitous motifs common to many RNA viruses. These structures function in numerous aspects of the life cycles of these viruses, including RNA replication and translation.

This project contains two major foci within the area of nodaviral RNA replication: (i) to elucidate the structural characteristics of a *cis*-acting element, 3'SL, that is required for RNA2 replication, including its potential inclusion in a predicted long-range tertiary structure element; and (ii) to determine the functional implications of another predicted stem-loop structure, 3'10SL, at the extreme 3'-end of the RNA2 genome segment Herein, we examine the mechanistic role of the individual components of the 3'SL that are responsible for RNA2 replication, specifically the double-stranded stem and the single-stranded loop. We demonstrate that each of these regions retains separate requirements for successfully directing RNA replication. We also illustrate that the NoV RNA2 3'SL functions in both strands of RNA2: the positive strand genomic RNA and the negative strand antigenomic RNA replication intermediate. This work examines the specific structural requirements of the NoV 3'SL in the context of full-length RNA2 in a mammalian system and its potential functions in RNA2 replication. It will also consider the role in RNA2 replication of a complex RNA tertiary structure in which the loop of 3'SL is predicted to base pair with a sequence over 600 nucleotides upstream. Additionally, our work herein demonstrates that the predicted 3'10SL at the extreme 3' end of RNA2 is at least partially responsible for protecting this genome segment from enzymatic modification and that it is potentially involved with RNA stability.

CHAPTER 2

BACKGROUND

2.1 Thermodynamics and RNA structure

The three-dimensional folding of RNA is largely, but not entirely, based upon thermodynamic stability (Tinoco Jr., *et al.*, 1971; Tinoco Jr. & Bustamante, 1999). The stabilizing forces generated by both canonical Watson-Crick and non-canonical G-U base-pairing interactions (Figure 1) help to preserve RNA structures, while the electrostatic repulsion between negatively charged phosphate residues of the backbone, as well as steric inhibition (torsion forces), lessen this effect (Varani and McClain, 2000).

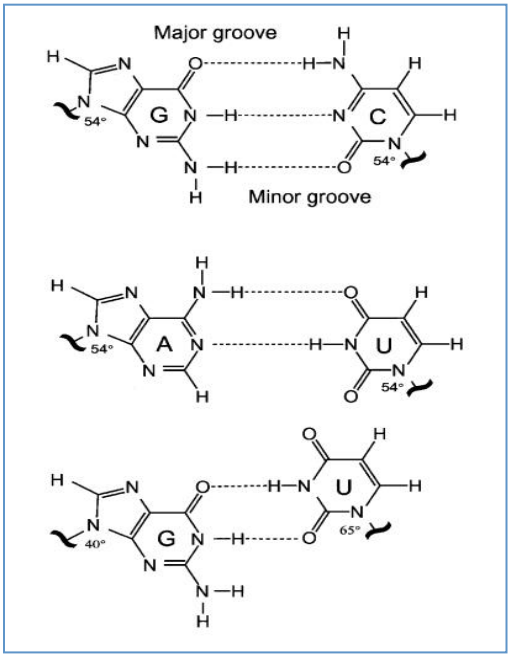

Figure 1: Typical base pairing interactions that form in RNA. Shown are three representations of base pairing that frequently occur in RNA. At top is a G-C bond, which forms three stable hydrogen bonds, making it the strongest of the three base pairs. In the middle, a weaker interaction is created by the base pairing of A and U, which form only two hydrogen bonds. At bottom is an RNA-typical G-U base pair, which is of similar strength to the A-U pair. Although G-U base pairing occurs only in RNA, it does so frequently and with high degrees of phylogenetic conservation (Varani and McClain, 2000). Figure from Varani and McClain, 2000.

As defined by the classical Gibb's free energy formulation, the decrease in entropy of the RNA molecule created by base-pairing interactions, multiplied by the absolute temperature of the system, must be less in magnitude than the enthalpy released by bond formation. Therefore, temperature and ionic strength of the solvent

solution remain critical factors in RNA structure formation. It is important to note that the most thermodynamically favorable structure may not be physiologically relevant: computer algorithms may calculate the minimum free energy of discrete structures, while not accounting for the kinetics of RNA folding or stability of structural resonance isoforms (Gardner and Giegerich, 2004).

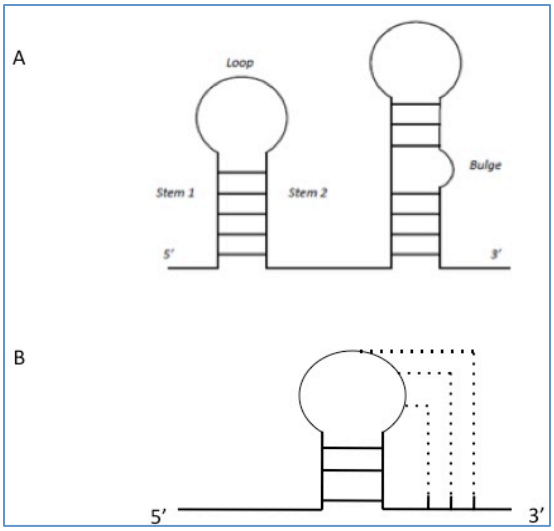

Figure 2: RNA folding is hierarchical. A, shown are two stem loops (SL's), which are common RNA secondary structures. Each structure is composed of double-stranded nucleotides forming the stem and an intervening sequence of single-stranded nucleotides that form the loop. Unpaired nucleotides in the stem create bulges, as shown at right. **B,** a simple depiction of an RNA pseudoknot. Pseudoknots are created when nucleotides in the loop of a SL base pair with nucleotides outside of the SL, either up- or, downstream. The SL must form first in order to present the loop for base pairing.

Analogous to protein folding, RNA folding is hierarchical (Figure 2) in that each level of folding introduces new interactions and vastly greater complexity to the molecule (reviewed by Brion and Westhof, 1997; Pleij *et al.,* 1985 and Tinoco Jr. & Bustamante, 1999). RNA primary structure consists of the sequence of nitrogenous bases (A, C, G, and U) in the RNA molecule. RNA secondary structures are composed of elements in a two-dimensional plane: single-stranded nucleotides and double-stranded (or base-paired) nucleotides. A simple secondary element is a stem-loop (SL), which forms when two regions of complementary sequence separated by at least three nucleotides base pair with one another; the intervening nucleotides form a single stranded loop (Figure 2A). Any nucleotide that does not have a base pairing partner in a stem is said to be a bulged nucleotide.

An RNA tertiary structure called a pseudoknot allows nucleotides in the single-stranded loop of a stem-loop structure to base pair with single-stranded nucleotides that lie either up- or downstream of the SL (Pleij, 1995). Pseudoknot structures (Figure 2B) were originally presented as regions of RNA that exhibited twisting of the helix to promote base pairing between two separate domains that do not share overlapping nucleotides (Studnicka *et al.*, 1978). More recently, pseudoknots have been defined as structures in which single-stranded nucleotides in the loop of an SL base pair with nucleotides outside of the SL (Pleij, 1990; ten Dam *et al.*, 1992; Wyatt *et al.*, 1990). Importantly, it is worth noting that the strands of the RNA duplex are not crossed as in a true knot, but rather the backbone is twisted to promote base pairing interactions among the substituent regions. The two stems of a pseudoknot form coaxial stacks of double-stranded RNA, which is thought to relieve torsional stress on the phosphate backbone yet allows the structure to retain the structural stability provided by base stacking (Holland *et a*l., 1999*;* Rietveld *et al.*, 1982).

Pseudoknots are transient structures, and in many cases, a pseudoknot will exhibit a dynamic equilibrium between its substituent SL's. Preliminary *in vitro* analysis of pseudoknots using short RNA oligonucleotides investigated the thermodynamic stability of these structures under varying ionic conditions (Wyatt *et al.*, 1990; reviewed by Draper, 1996), while the *in vivo* functions of these structures were not elucidated until more recently. Tertiary and quaternary nucleic acid structures involve the interactions of multiple secondary structures and RNA molecules, respectively (Brion and Westhof, 1997). These levels of RNA folding must occur in a three-dimensional space, as all

previous folding is accomplished in only two-dimensions. Common quaternary structures are generally created through either RNA-RNA or RNA-protein interactions.

While it is feasible to predict RNA secondary and tertiary structures using computational methods or by identification of sequences that are phylogenetically conserved with structures that have been predicted or shown to form empirically, many sources have reported the transience of tertiary structure formation, which itself is highly dependent on the ionic content of the solution (Draper, 2008; Lambert *et al.*, 2009; Tan and Chen, 2011). Higher ionic concentrations of Na^{+}, Mg^{2+}, and other mono- and multivalent cations lead to greater stability in RNA tertiary structures. This is accomplished by site-specific binding of coordinated ion-complexes that act to buffer the electrostatic charge of nearby phosphate residues. Under biological conditions, pseudoknots are naturally flexible RNA structures. This structural plasticity allows for multiple conformations, or resonance forms, between the substituent stem loops and the intermediate pseudoknot. One of the common models of pseudoknot formation posits that the two regions of double-stranded RNA that form the stems, are linked by two regions of single stranded RNA, the loops, and may stack coaxially to promote stability (Pleij *et al.*, 1985). In addition to the aforementioned resonance between substituent structures and pseudoknot formation, the instability of RNA tertiary interactions also has functional implications (Oltshoorn, *et al.*, 1999). The flexible nature of RNA structures allows for several forms to be present, although not concurrently, regulating various aspects of RNA replication (Klovins and Van Duin, 1999).

While computer modeling provides an excellent foundation upon which to base investigations, RNA structures verified *in vitro* often deviate from the structure with the

lowest predicted minimum free energy value. Therefore, empirically determining the nature of every thermodynamically predicted structure is critical for validation of any computationally derived model. Experimental analysis of these structures is generally accomplished through several methods, the first of which is covariation mutagenesis. Nucleotides that are suspected of participating in structural interactions are mutated so as to inhibit structure formation and the phenotypic effects of these mutations are then examined. If these mutations are deleterious because an important structural element has been disrupted, we predict that the mutant phenotype could be restored to a wildtype (WT)-like phenotype through the use of compensatory mutations that restore base pairing with alternative complementary sequences. If the primary sequence is the more important determinant, we predict that compensatory mutations will not restore the phenotype. This concept is explored further in the Results section.

Chemical and enzymatic probing provides a valuable tool in structure determination. RNAs are treated with either a chemical or ribonuclease that specifically modifies or cleaves the target RNA at specific positions (Doris-Keller *et. al.,* 1977; Inoue and Cech, 1985; reviewed by Ehresmann *et al.*, 1987; Weeks, 2010; Table 2). End-labeled RNAs can be directly analyzed by denaturing polyacrylamide gel electrophoresis (PAGE), while unlabeled RNAs can be analyzed by primer extension using labeled primers or by Northern blot hybridization with labeled riboprobes (Hanley *et al.,* 1992; Romero *et al.,* 2006; Rosskopf *et al.*, 2010; Tuplin *et al.*, 2004). Treatment of RNAs with ribonuclease T1, for example, will selectively cleave the phosphodiester bond of the RNA 3' to single-stranded guanine residues, while addition of dimethyl sulfate ($C_2H_6O_4S$) causes adenosine, cytosine, and guanine residues to become

methylated, which act as a steric blocks during subsequent primer extension reactions (Peattie and Gilbert, 1980; Tijerina *et al*., 2007). Table 2 provides select examples of several enzymes and chemicals used in RNA structure probing and their target nucleotides.

Table 2: Select enzymatic and chemical probes used to determine RNA structure.

RNase / Chemical	Target Nucleotide
RNase T_1	ss G
RNase U_2	ss A (May cleave other residues)
RNase V_1	ds RNA
RNase S_1	ss RNA
Dimethyl sulfate (DMS)	Methylates A, C, G residues
β-etoxy-α-ketobutyraldehyde (kethoxal)	Creates adducts on G residues

ss, single-stranded; ds, double-stranded

In-line structure probing has also proven to be a useful technique in elucidating RNA structural composition. This method takes advantage of the highly reactive 2'-hydroxyl (OH) group specific to RNA and its ability to participate in transesterification reactions with the phosphate group 3' to the ribose sugar (Soukup and Breaker, 1999). Because single-stranded nucleotides are more susceptible to these nucleophilic attacks than are double-stranded nucleotides, for which hydrogen bonding between complementary bases inhibits transesterification (Soukup and Breaker, 1999), in-line structure probing allows the verification of which bases are most likely single-stranded. Furthermore, greater resolution can be achieved when the in-line method is used in conjunction with a base-specific nuclease or with alkaline conditions, which catalyze the cleavage of the phosphodiester bond (McCormack *et al*., 2008; Winkler *et al.,* 2002),

Indeed, in-line probing has recently been used to elucidate structures in the 3' UTR of *Turnip crinkle virus*, validating this method's efficacy in evaluating viral RNA structures (McCormack *et al*., 2008).

2.2 Viral RNA structure and function

The function of RNA is often determined by its structure. Viral RNA structures play key roles in regulating numerous phases of the viral replication cycle, including genome replication, transcription, translation and packaging, and increasingly, we are discovering the multifaceted functions of RNA (Brierley et al., 2007). Our understanding of the regulatory and enzymatic functions that viral RNAs play during infection can lead to discovery of new therapeutic targets, new methods of viral attenuation, potential targets for novel vector creation, and a greater understanding of how our own RNAs function in the cell. For example, pseudoknots in viral genomic or subgenomic RNAs play roles in ribosomal frame shifting, internal ribosome entry, transcriptional regulation, and genome replication (reviewed by Brierley *et al.*, 2007; Deiman & Pleij, 1997; Westhof & Jaeger, 1992).

Many positive-strand RNA viruses contain highly structured UTRs at both the 5' and 3' termini of their genomes. Important preliminary investigations of viral RNA (vRNA) structure concerned the 3' UTRs of positive-strand RNA plant virus genomes. In 1970, it was discovered that the *Turnip yellow mosaic virus* genome is valine-aminoacylatable *in vitro* (Pinck et al., 1970; Yot et al., 1970). It rapidly became clear that numerous other positive-strand RNA plant virus genomes, including those of members of the *Cucumo*-, *Bromo*-, *Tymo*- and *Tobamovirus* genera are similarly reactable.

Pseudoknot structures at the 3' end of the genome behave as tRNA mimics, interacting with numerous tRNA-related enzymes (e.g. aminoacyl tRNA synthetases, tRNA nucleotidyl transferases, translation factors, etc.), and were therefore deemed tRNA-like structures (TLS's). While many studies noted that the primary sequences and secondary structures of these tRNA mimics differed among viruses, all found that TLSs functioned similarly, playing critical roles in aminoacylation of the genome and negative-strand synthesis (Morch et al., 1987; reviewed by Giegé et al., 1993 and Mans et al., 1991). For reviews on the tRNA-like structures of positive-strand RNA plant viruses, please see Dreher, 2009; Joshi *et al.*, 1983; Mans *et al.*, 1991; Rietveld *et al.*, 1983.

Structural elements in virion RNA (vRNA) have also been implicated in aiding genome replication in animal viruses from numerous virus families, including the *Picornaviridae* (Melchers *et al.*, 1997; Miller *et al.*, 1986; Rohll *et al.*, 1995), *Coronaviridae* (Williams *et al.*, 1999), *Leviviridae* (Klovins & van Duin, 1998, 1999), and *Flaviviridae* (Shi *et al.*, 1996; Tilgner & Shi, 2004; reviewed by Liu *et al.*, 2009). More recently, these RNA structural elements have been renamed *cis*-acting replication elements. By definition, a *cis*-acting replication element directs replication of the molecule that contains it, i.e., *in cis*; its function cannot be provided by a copy of the same sequence provided by another RNA molecule *in trans* (Liu *et al.*, 2009). For some viruses, pseudoknot structures have been shown to play the role of a molecular switch, either turning replication ON or OFF depending on which structural resonance form is present (Olsthoorn *et al.*, 1999). Others have shown the importance of pseudoknot formation for both genome replication and independent enzymatic activity, indicating that pseudoknots may play numerous roles during active viral replication (Jeng *et al.,*

1996). The present study aims to elucidate how RNA structural elements regulate viral RNA replication for *Nodamura virus.*

2.3 *Nodamura virus* biology

Nodamura virus (NoV) is the first described member and type species, the designated virus after which the family is named, of the *Alphanodavirus* genus of the virus family *Nodaviridae* (Scherer and Hurlbut, 1967; Thiery *et al*., 1998). NoV was first isolated in the village of Nodamura, Japan, in 1956 during a screen for Japanese encephalitis virus (Scherer and Hurlbut, 1967; Ball and Johnson, 1998). It soon became apparent that it was distinct from all known virus families so became the first species in a new family, the *Nodaviridae*.

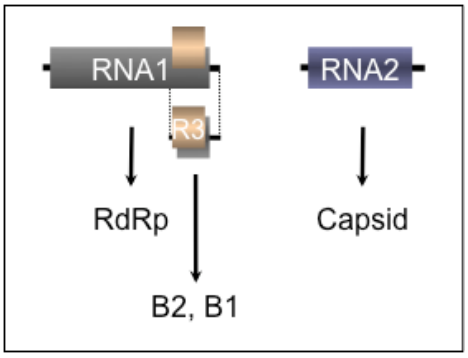

Figure 3: Genome organization of the *Nodaviridae.* Shown is a schematic of the nodavirus RNA genome. RNA1, ~3.2 kb, encodes the multifunctional RNA-dependent RNA polymerase (RdRp). RNA3 (470 nt), 3'-coterminal with RNA1, is synthesized by the RdRp from an RNA1 template during RNA replication. RNA3 encodes proteins B2, a suppressor of host RNA interference (RNAi) responses, and B1, whose function is unknown. RNA2, ~1.3kb, encodes the structural protein precursor that is autocatalytically cleaved after particle assembly to yield the capsid proteins found in the mature virion.

NoV contains a small (approximately 4.5 kb), bipartite, positive strand RNA genome, shown schematically in Figure 3. Unlike mammalian RNAs, which contain trimethylated ^{7}mGpppNmpNmp-RNA cap-2 structures (Decroly *et al.*, 2012) and poly-A tails, the termini of both nodavirus genome segments and of RNA3 contain a

monomethylated 5' ^{7}mGpppNp (cap-0) structure and lack poly-A tails (Dasgupta and Sgro, 1984; Newman and Brown, 1976).

The nodavirus RNA replication and packaging functions are naturally segregated onto separate RNA molecules: genomic RNA1 and RNA2, respectively. NoV RNA1 (3204 nucleotides) encodes the multifunctional Protein A, the viral contribution to the RNA-dependent RNA-polymerase (RdRp) that replicates both genomic RNAs and subgenomic RNA3 (Ball and Johnson, 1998). This protein is predicted to contain a guanylyltransferase activity that may synthesize the 5' caps found on both genomic and subgenomic RNAs (Johnson *et al.* 2001). It also participates in the formation of the RNA replication complexes that are the sites of RNA replication in the cell, in association with cellular membranes (Kopek *et al.*, 2010; Van Wynesberghe and Ahlquist, 2009; Gant *et al.,* manuscript in preparation). During the process of RNA replication, positive strand genomic RNAs are copied into negative strand RNA replication intermediates, which are used as templates for further positive strand synthesis. The products of RNA replication include both monomeric and dimeric forms of the genomic and subgenomic RNAs (Albariño *et al.*, 2001; Eckerle and Ball, 2002; Price *et al.*, 2005; Rosskopf *et al.*, 2010). We and others have proposed that these negative strand dimers may be the templates from which monomeric positive strand RNAs are synthesized (Albariño *et al.*, 2001; Rosskopf *et al.*, 2010). This hypothesis predicts that the RdRp may recognize an internal *cis*-acting signal near the dimer junction and initiate transcription of a monomeric positive strand RNA. However, it also remains possible that the dimers represent dead-end products that do not play a further role in the viral life cycle.

During RNA replication, a small subgenomic RNA, RNA3, is synthesized from RNA1 (Figure 3). Subgenomic RNAs are defined as RNAs smaller than genome length that are transcribed from genomic RNAs by the viral RdRp but are not packaged into viral particles (Miller and Koev, 2000); subgenomic RNAs allow translation of ORF's that are internal to the genomic RNAs. While NoV genomic RNAs 1 and 2 are co-packaged into the same virion, subgenomic RNA3 is not packaged (Newman and Brown, 1977; Friesen and Rueckert, 1981, 1982).

For NoV, subgenomic RNA3 is 3' co-terminal with the last 470 nucleotides of RNA1 and contains two overlapping open reading frames (ORFs) that encode proteins B1 and B2 (Johnson *et al.*, 2001, 2003). While the function of B1 remains unknown, the B2 proteins of both NoV and the related alphanodavirus *Flock House virus* (FHV) suppress RNA interference (RNAi) responses in plant, insect and mammalian cells (Johnson *et al.*, 2004; Li *et al.*, 2002; Li *et al.*, 2004; Sullivan and Ganem, 2005). Studies of FHV B2 suggest that it may function by binding to both viral double-stranded RNA, such as the replicative intermediate, and to virus-derived siRNAs (Chao *et al.*, 2005; Kürber *et al.*, 2009), thus sequestering them from host innate antiviral defenses. For FHV, RNA3 synthesis is dependent upon intramolecular long distance base-pairing interactions in RNA1 (Lindenbach *et al.*, 2002), although the mechanistic significance of this structure in RNA3 synthesis remains to be determined. And for FHV, the RdRp replicates RNA3 via complementary strand intermediates, which explains the presence of both positive- and negative-strand forms of RNA3 in infected or transfected cells (Eckerle *et al.*, 2002; Zhong and Rueckert, 1993).

RNA2 (1336 nucleotides) encodes Protein α, the capsid protein precursor (Newman *et al.*, 1978). This precursor is autocatalytically cleaved upon virion maturation to yield proteins β and γ, which remain associated in the infectious particle, along with detectable levels of the precursor α (Friesen and Rueckert, 1981; Johnson and Reddy, 1998). Replication of RNA2 requires RNA3 *in trans* independently of proteins B1 and B2, while RNA3 synthesis is inhibited by RNA2 (Albariño *et al.*, 2001, 2003; Eckerle and Ball, 2002; Eckerle *et al.*, 2003; Zhong and Rueckert, 1993). It was proposed that this counter-regulation is required to coordinate the replication of genomic RNA1 and RNA2 segments so that they are synthesized in equimolar amounts, thereby facilitating their packaging at a 1:1 molar ratio (Eckerle and Ball, 2002; Eckerle *et al.*, 2003).

2.4 Nodaviruses and RNA structure

In 1990, the genomic RNAs of the four known alphanodaviruses, namely FHV, *Black beetle virus* (BBV), *Boolarra virus* (BoV) and NoV, were subjected to computer RNA structure prediction analysis with mfold, which folds RNA using predictive algorithms that are based on minimum free energy configurations (Zuker & Stiegler, 1981). The results of the predictions suggested the presence of RNA secondary structures in the 3' UTRs of the genomic RNAs of these viruses (Kaesberg *et al.*, 1990). Interestingly, the 3'-terminal 50 nucleotides of the RNA2 segments of FHV, BBV and BoV were predicted to fold into similar structural arrangements (Figure 4).

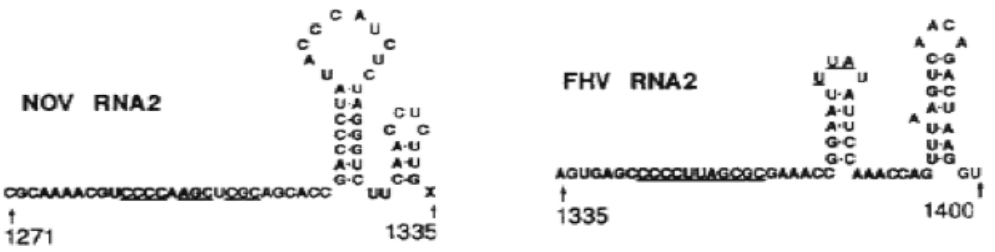

Figure 4: Possible secondary structures in the 3' UTR of nodavirus RNA2 segments, as predicted by minimum free energy conformation. The 3'-terminal 50 nucleotides of four nodaviruses were folded predicted with mfold software. At left is the predicted structure for NoV RNA2, which was predicted to fold differently from the other three alphanodaviruses, represented at right by the prediction for FHV RNA2. The underlined sequences 5' adjacent to the upstream stem loop indicate conserved residues in the genome. Reproduced from *Kaesberg et al., 1990.*

These RNA2 segments were predicted to form two stem loop structures in their respective 3'-UTRs, with the smaller of the two structures upstream of the larger. In contrast, NoV RNA2 was predicted to have the smaller structure positioned downstream of the larger stem loop, near its 3'-terminus. Kaesberg *et al.* (1990) posited that it was this structural divergence that account for the inability of NoV genomic RNAs to cross replicate with genome segments from the other alphanodaviruses, as described by Gallagher (1987). Additionally, it was proposed that this UTR might have a functional role in RNA replication initiation.

RNA replication studies with FHV identified a presumptive *cis*-acting RNA replication element within the 3'-terminal 50 nucleotides of RNA2 (Albariño *et al.*, 2003). This short sequence was responsible for, at least in part, directing replication of a chimeric RNA2 molecule that contained a heterologous sequence derived from yellow fluorescent protein (YFP), as mutants lacking these nucleotides failed to serve as viable templates for RNA replication (Albariño *et al.*, 2003). These lines of evidence highlighted the potential importance of this region in RNA replication.

The availability of powerful RNA structure prediction software capable of predicting the presence of pseudoknots (Pknots-RG [Reeder & Giegerich, 2004], Pknots-RE [Rivas & Eddy, 1999] and NuPack [Dirks & Pierce, 2003, 2004]) led us to revisit the prediction of RNA secondary and tertiary structures in the RNA2 3'UTR's. We and our collaborators used these tools to predict the formation of more complex structures 3'UTR of five alphanodaviruses, including BBV, BoV, FHV, NoV and *Pariacoto virus* (PaV) (Johnson *et al.*, 2000; Zeddam *et al.*, 1999), and two betanodaviruses, *Striped jack nervous necrosis virus* (SJNVV) and *Greasy grouper nervous necrosis virus* (GGNNV) (Taufer *et al.*, 2008).

In this investigation, we used Pknots-RG (Reeder & Giegerich, 2004), Pknots-RE (Rivas & Eddy, 1999) and NuPack (Dirks & Pierce, 2003, 2004) software to fold the 3'-terminal 100 nucleotides of each viral RNA2 molecule. Interestingly, all of the viruses considered showed conservation of a 3' UTR stem loop structure, and five of the seven viruses (FHV, BoV, PaV, SJNNV and GGNNV) predicted pseudoknot formation, while neither NoV nor BBV was suggested to form a pseudoknot (Figure 5). Interestingly, NoV RNA2 was predicted to contain a pseudoknot when a larger sequence from RNA2 was folded (Taufer et al. 2008). In addition, our recent work has predicted a long-range base-pairing interaction between the 3'SL and another RNA sequences over 600 nucleotides apart (Johnson and Leung, in preparation). Nevertheless, this study suggests that the presence of RNA tertiary structures occurring in the 3' UTR is a conserved feature across most of the *Nodaviridae,* and that the presence of a stem loop in this region may indeed have functional implications in RNA replication (Taufer *et al.*, 2008). Additionally, in contrast to the study by Kaesberg *et al.* (1990), the work by

Taufer et al. (2008) predicted only a single stem loop in the 3'UTR of NoV RNA2, (Figures 4 and 5), although the structure previously predicted for BBV was recapitulated.

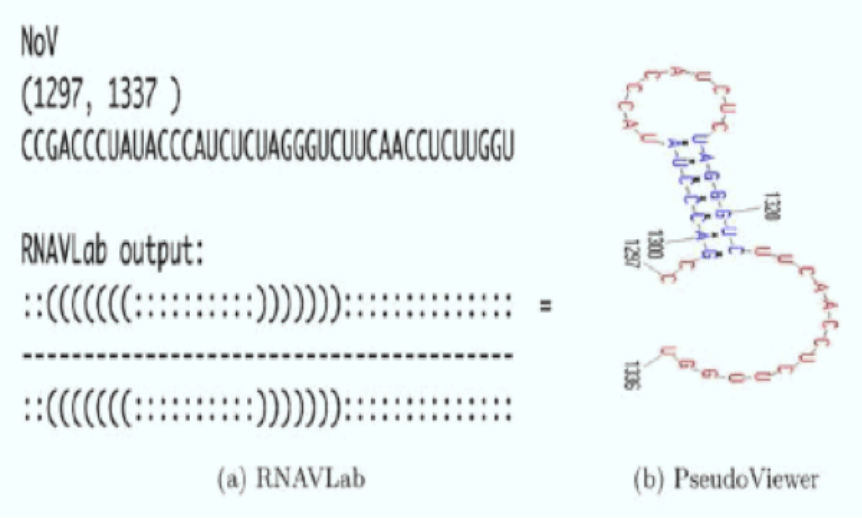

Figure 5: Predicted structure of the NoV RNA2 3'-terminal 100 nucleotides. Three programs able to predict pseudoknots were used to identify common motifs in the 3'-terminal 100 nucleotides of seven nodavirus RNA2 segments. A single SL predicted for NoV forms the basis for a pseudoknot in five of the others. These algorithms did not predict the 3'-terminal SL described by *Kaesberg et al.(1990).* Figure reproduced from Taufer et al., 2008.

Most recently, work from our laboratory experimentally confirmed the presence of the NoV RNA2 stem loop, 3'SL, in solution using nuclease mapping (Rosskopf *et al.,* 2010). The structure probing showed an 86% correlation with the predicted structure, suggesting it is likely to form. To determine whether the predicted structure played a role in the viral life cycle, we relied on our ability to construct replicons based on RNA2. These are small RNA elements that can be replicated by the RdRp *in trans*. We showed previously that a large portion of NoV RNA2 could be deleted without loss of RNA replication activity and that these RNA2 sequences could be replaced with heterologous RNA sequences such as the yeast *HIS3* and *URA3* genes and green fluorescent protein (GFP; Price *et al.* 2005; Rosskopf *et al.* 2010). The resulting RNA2-based replicons could replicate in the presence of the RdRp as long as the heterologous RNA sequences were flanked by the 5' and 3' ends of NoV RNA2, which must therefore

contain essential *cis*-acting RNA replication signals. These replicons functioned both in yeast and in transfected mammalian cells (Price *et al.* 2005 and Johnson, Price and Ball, unpublished, respectively).

For the purpose of testing the role of the 3'SL in the viral life cycle, we constructed the replicons shown schematically in Figure 6. These replicons all contained the seventeen (17) 5'-terminal nucleotides of RNA2, and the ORF of green fluorescent protein, which provided a site to which strand-specific probes could be directed that was common to all of the replicons. However, they differed in the extent of RNA2 sequence at their 3' termini. The larger parental replicon contained the 236-most 3'-terminal nucleotides of RNA2, which had been shown previously to be sufficient for RNA replication (Price *et al.*, 2005; Johnson and Ball, unpublished data).

Deleting the 24 nucleotides that comprise the 3'SL from this replicon severely inhibited RNA replication, affecting both positive and negative strand synthesis. Importantly, deletion of the stem loop resulted in high levels of accumulation of negative strand RNA2 dimers, possibly by precluding the copying of the dimers to yield monomeric positive strand RNA2 species.

To determine whether only the nucleotides that form the 3'SL were sufficient to direct RNA replication, we constructed a minimal replicon that retained only the 54-most 3'-terminal nucleotides of RNA2. This replicon was capable of synthesizing both positive and negative strand RNA replication products, albeit at a level that was about 30% as much as the parental replicon, a level which we termed "basal replication". The parental replicon, in turn, replicated less well than full-length RNA2, which may suggest that additional sequences are required for optimal levels of RNA2 replication.

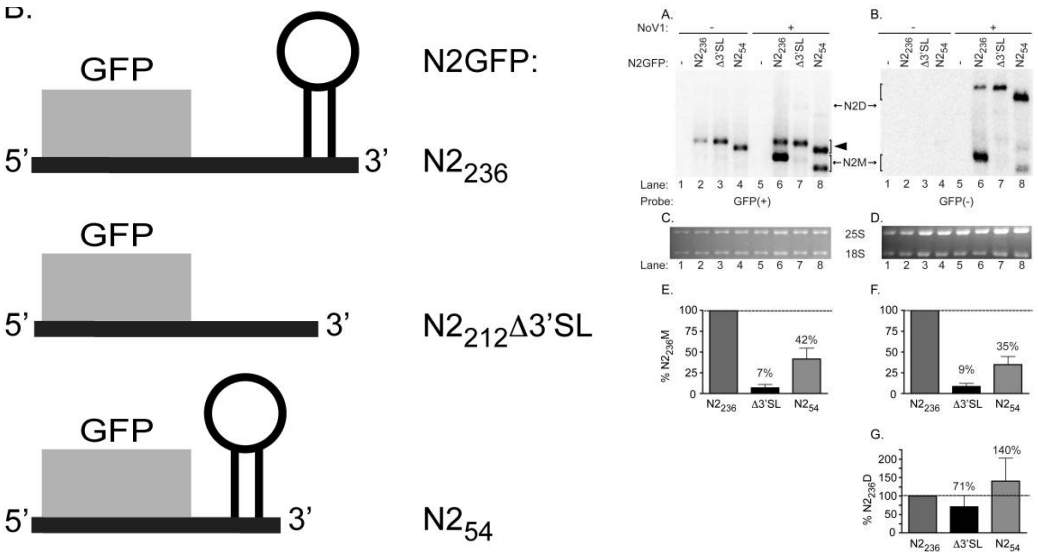

Figure 6: NoV RNA2 based replicons require the presence of the 3'SL to replicate. Shown at left are schematics of the replicons described in Rosskopf *et al.* (2010). All constructs contain the 5'-terminal 17 nucleotides of NoV RNA2, followed by the GFP central core and either 236, 212 or 54 nucleotides from the 3'- end of RNA2. At right, Northern blot hybridization was used to detect the positive or negative strand RNA replication products of the replicons (A and B, respectively). Importantly, deleting 3'SL from these replicons led to severe decreases in synthesis of positive and negative strand monomers (Blot A, Lane 7), yet did not preclude formation of the negative strand dimer (Blot B, Lane 7). This suggested that 3'SL may be involved in the production of monomeric positive strands from dimeric replication intermediates. The bolded arrow represents primary transcripts by the T7 RNA polymerase in which the hepatitis delta virus antigenomic ribozyme failed to cleave. Taken from *Rosskopf et al., 2010.*

This work suggests that the 3'SL plays an important role in regulating RNA2 replication. Exactly how the 3'SL functions is yet unclear, although we hypothesize that it may be involved in RNA-RNA or RNA-protein interactions responsible for coordinating RNA replication. The work conducted here defines which elements of the 3'SL are critical for RNA replication. Although the presence of the 3'SL had been computationally predicted for over twenty years (Kaesberg *et al*, 1990), its role in the viral life cycle remained to be determined. Our more recent work showed the structure to be conserved across both genera of the *Nodaviridae* (Taufer *et al*, 2008), and its presence been verified experimentally (Rosskopf *et al*, 2010). We hypothesize that the

3'SL functions to make accessible the loop sequences to an as yet unidentified factor (RNA or protein) that is critical for viral RNA replication. In our hypothesis, the stem region of 3'SL functions as a structural scaffold to present the loop to this factor. We show here that the sole requirement of the stem is base pairing to provide structural support. As such, the sequence and length of the stem remain mutable characteristics for RNA replication. Additionally, we illustrate that the loop of 3'SL retains strict sequence and structural requirements for RNA replication. Further, we implicate another *cis*-acting signal approximately 650 nucleotides upstream of 3'SL in RNA replication. Here, we show that each component of the stem loop retains separate requirements that enable successful RNA replication. While we have characterized the functional and structural characteristics of the 3'SL in RNA replication, the bioinformatic approaches used in our investigations indicated other SL structures may be present in WT RNA2, and we therefore asked whether these structures also play functional roles in the NoV replication cycle.

2.5 Non-reactivity of nodaviral RNA 3'-termini to enzymatic modification

The 3' ends of nodaviral RNAs are non-reactive to 3'-termini modifying enzymes (Guarino *et al*., 1984; Dasgupta and Sgro, 1984; Dasmahapatra *et al*., 1985). The 3'-termini of both genomic and subgenomic RNAs of BBV are resistant to modification with bacteriophage T4 RNA ligase and *E. coli* poly(A) polymerase enzymes (Guarino *et al.*, 1984; Dasgupta and Sgro, 1984; Dasmahapatra *et al.*, 1985). Similarly, it was suggested but not shown that the 3'-termini of RNA2 from NoV, FHV and BoV are also blocked from modification (Kaesberg *et al.*, 1990). It was originally proposed that a

protein was bound to the 3'-terminus, blocking modification by functionally removing the 3'-hydroxyl (Dasmahapatra *et al.*, 1985). However, no cellular or viral protein has been found to be covalently attached to the 3'-terminus of nodavirus genomic RNAs. The 3'-end of many positive strand RNA viruses is involved in complex secondary and tertiary RNA structures. Viral RNA is less prone to modification or degradation if the 3'-terminal reactive hydroxyl is recessed or hidden. Kaesberg *et al.* (1990) predicted the formation of another stem-loop structure (3'10SL) at the extreme 3'-terminus of NoV RNA2. As described in the Results chapter, we hypothesize that 3'10SL may act as a structural shield, protecting the 3' end of the viral genome from degradation or other enzymatic modification.

CHAPTER 3

MATERIALS AND METHODS

3.1 Cells and viruses

All RNA replication studies were performed in BSR-T7/5 cells, which are baby hamster kidney BHK21 cell derivatives that constitutively express T7 RNA polymerase (Buchholz, 1997). Cells were grown at 37^{o}C under 5% CO_2 in complete Glasgow's Minimum Essential Media (cGMEM), supplemented with 5% fetal bovine serum, 5% newborn calf serum, 3.4% tryptose phosphate broth, 5 mL of PenStrep (Gibco) and 1 mg/mL g418 (Invitrogen). Transfections were conducted using Lipofectamine 2000 (Invitrogen) according to manufacturer's instructions, in the presence or absence of 2.5 μg of plasmid pNoV1 (provided as a source of RdRp *in trans*) and 1.0 μg of either WT RNA2 or mutant pNoV2. Cells were incubated for 4 hours at 28^{o}C, whereupon the transfectant was aspirated and replaced with cGMEM supplemented with g418, and incubated for another 20 hours. All plasmids were amplified in the NEB-5α strain of E. coli (New England Biolabs).

3.2 Plasmids

Plasmids pNoV1 and pNoV2 contain cDNA clones of NoV genomic RNA1 or RNA2, respectively, under transcriptional control of bacteriophage T7 promoters (Johnson *et al.*, 2003). Mutations were generated by circular PCR-based mutagenesis followed by *DpnI* selection (Sambrook and Russell, 2001), using pNoV2 as a template and the outward-facing primer pairs shown in Table 3; the method is shown schematically in Figure 7. This method can be used to generate substitutions, deletions, or insertions,

depending on the sequences of the primers used. Briefly, complementary pairs of mutagenic primers that contain the desired mutation are used to amplify the entire template plasmid. The resulting reaction mixture will contain both the parental plasmid, which was methylated during its original amplification in *E. coli*, and the unmethylated plasmid generated during the PCR reaction.

Table 3: Primers used in this study

Purpose	Primer	Sequence
Mutagenesis	S1-up(+)	CGTCCCCAAGCTCGTAGCACCCTGGGATTACCCATCTCTAGGGTCTTCAACCTCT
	(-)up-S1	CGACCCACCAAGAGGTTGAAGACCCTAGAGATGGGTAATCCCAGGGTGCTACGA
	S2-down(+)	CGTCCCCAAGCTCGTAGCACCGACCCTATACCCATCTCATCCCAGTTCAACCTCT
	(-)down-S2	CGACCCACCAAGAGGTTGAACTGGGATGAGATGGGTATAGGGTCGGTGCTACGA
	S1S2-dbl(+)	CGTCCCCAAGCTCGTAGCACCCTGGGATTACCCATCTCATCCCAGTTCAACCTCT
	(-)dbl-S1S2	CGACCCACCAAGAGGTTGAACTGGGATGAGATGGGTAATCCCAGGGTGCTACGA
	Pos-S2(+)	CGTCCCCAAGCTCGTAGCACCGACCCTATACCCATCTCTAAAATCTTCAACCTCT
	MinusS2(+)	CGACCCACCAAGAGGTTGAAGATTTTAGAGATGGGTATAGGGTCGGTGCTACGA
	Neg-S1(+)	CGTCCCCAAGCTCGTAGCACCGATTTTATACCCATCTCTAGGGTCTTCAACCTCT
	(-)S1-neg	CGACCCACCAAGAGGTTGAAGACCCTAGAGATGGGTATAAAATCGGTGCTACGA
	Loopdel(+)	CGTCCCCAAGCTCGTAGCACCGACCCTATAGGGTCTTCAACCTCTTGGTGGGTC
	(-)loopdel	CGACCCACCAAGAGGTTGAAGACCCTATAGGGTCGGTGCTACGAGCTTGGGGAC
	Looptrans(+)	CGTCCCCAAGCTCGTAGCACCGACCCTAGCAAACGAGATAGGGTCTTCAACCTCT
	(-)looptrans	CGACCCACCAAGAGGTTGAAGACCCTATCTCGTTTGCTAGGGTCGGTGCTACGA
	4loop(+)	CGTCCCCAAGCTCGTAGCACCGACCCTAGAGATAGGGTCTTCAACCTCTTGGTGC
	(-)4loop	CGACCCACCAAGAGGTTGAAGACCCTATCTCTAGGGTCGGTGCTACGAGCTTGG
	3loop(+)	CGTCCCCAAGCTCGTAGCACCGACCCTATCATAGGGTCTTCAACCTCTTGGTGGC
	(-)3loop	CGACCCACCAAGAGGTTGAAGACCCTATGATAGGGTCGGTGCTACGAGCTTGGG
	delSL(+)	GCGTTGACGACGCAAAACGTCCCCAAGCTCGTAGCACCTTCAACCTCTTGGTGGC
	(-)DelSL	CGACCCACCAAGAGGTTGACATGCCGACCCACCAAGAGGTTGAAGGTGCTACGA
	deltaSL(+)	CGTCCCCAAGCTCGTAGCACCTTCAACCTTCAACCTCTTGGTGGGTCG
	(-)deltaSL	CGACCCACCAAGAGGTTGAAGGTGCTACGAGCTTGGGGACG
	S1Tv2(+)	CGTCCCCAAGCTCGTAGCACCTCAAAGCTACCCATCTCTAGGGTCTTCAACCTCT
	(-)S1Tv2	CGACCCACCAAGAGGTTGAAGACCCTAGAGATGGGTAGCTTTGAGGTGCTACGA
	S2Tv2(+)	CGTCCCCAAGCTCGTAGCACCGACCCTATACCCATCTCGCTTTGATTCAACCTCT
	(-)S2Tv2	CGACCCACCAAGAGGTTGAATCAAAGCGAGATGGGTATAGGGTCGGTGCTACGA
	655Tv2(+)	CCGTACCACCTACCAACTTGGCTCAGAACACAATTGCAATTTGCTCACTAGAAGC
	(-)655Tv2	CCGGAGTAGTTGTTATTTGGTAGTGCATCTAACGCTTCTAGTGAGCAAATTGCAA
	DSTv2(+)	CGTCCCCAAGCTCGTAGCACCTCAAAGCTACCCATCTCGCTTTGATTCAACCTCT
	(-)DSTv2	CGACCCACCAAGAGGTTGAATCAAAGCGAGATGGGTAGCTTTGAGGTGCTACGA
	Δ655v2(+)	GCTCAGAACACAATTGCAATACTAGAAGCGTTAGATGCACTACC
	(-)Δ655v2	GGTAGTGCATCTAACGCTTCTAGTATTGCAATTGTGTTCTGAGC
Sequencing	SP6recessed	GGCTTGTACATATTGTCGTTAGAACGCGG
	T7recessed	GGAAGCGGAAGAGCGCCC
	N1-1425	GGCATAAGCCCTGAGCCGTTTTCCAGG
RT	NoV2 5'T7	GCTCTAGACGTCTCGTATA GTAAACAACCAATAACATCATGGTATCC
	NoV2 3' Rz	GCTCTAGACGTCTCCACCCACCAAGAGGTTGAAGACCCTAGAGATG

The two plasmids (parental vs mutated daughter plasmid) can be separated by subsequent cleavage by the methylation-sensitive restriction endonuclease *DpnI*, which cuts the fully methylated parental plasmid but leaves the mutated daughter plasmids intact. The *DpnI*-treated plasmid mixture is amplified in *E. coli* and restriction mapping and DNA sequencing are used to confirm the presence of the desired mutation.

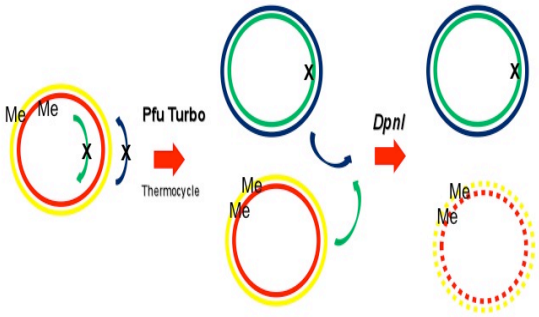

Figure 7: Generation of mutations used in this study were generated by circular PCR-based mutagenesis followed by *DpnI* digestion. The desired mutations were introduced into the NoV RNA2 cDNA by circular PCR-based mutagenesis followed by *DpnI* selection (Sambrook and Russell, 2001). Importantly, the PCR product is unmethylated because the thermostable DNA-dependent DNA polymerase (PfuTurbo) lacks methyltransferase activity. Following the PCR, plasmids were digested with the restriction endonuclese *DpnI*, which selectively cleaves its recognition sequence only when it is methylated, which occurs when a plasmid is amplified in *E. coli* (New England Biolabs). This digestion allows for the selection of plasmids containing the desired mutations for transformation into *E. coli*. Figure adapted from V.U.Gant's doctoral dissertation proposal.

For each construct, a small fragment containing the desired mutation was re-introduced into another copy of parental pNoV2 to ensure that no unintended mutations were introduced during the mutagenesis. For 3'SL and 3'10SL mutations, mutated plasmids were digested with *EagI* and *RsrII*, releasing a small (approximately 450 bp) fragment that was inserted into a similarly digested pNoV2 backbone, while the predicted upstream region (UR) mutations were introduced by digesting both the mutated and parental plasmids with *BsaI* and *EagI*.

3.3 RNA isolation and Northern blot hybridization analysis

Total cellular RNA was isolated from transfected BSR-T7/5 cells using an RNeasy Mini Kit (QIAGEN) and its concentration was determined using a Spectramax 100 plate reader. For Northern blot hybridization, equal amounts of total RNA were separated on denaturing formaldehyde-agarose gels (Lehrach *et al.*, 1977), 0.5 μg for detection of positive strands or 2.0 μg for detection of negative strands, and transferred to charged nylon membranes (Thomas, 1980). RNA replication products were detected with ^{32}P-labeled riboprobes specific for the positive or negative strands of NoV RNA2, as previously described (Price *et al.*, 2005; Rosskopf *et al.*, 2010). These species were visualized with a Personal Molecular Imager (Bio-Rad) and quantitated using Quantity One 1D Analysis Software (Bio-Rad).

Levels of RNA2 replication products were normalized to those of mammalian 28S ribosomal RNA (visualized by ethidium bromide staining of the gel before transfer) and are presented as a percentage of the WT RNA2 values. The relative RNA values from at least three independent experiments are presented as mean values ± standard deviations. Statistical significance was calculated with a two-tailed paired t test or one-way ANOVA with a post hoc Tukey's range test (Tukey, 1977) when considering several mutants concurrently.

3.4 Reverse transcription and cDNA synthesis

One microgram of total cellular RNA from cells transfected with plasmids pNoV1 and mutagenized pNoV2 was subjected to reverse transcription using SuperScript III (Invitrogen) according to manufacturer's instructions, using primers NoV2 5'T7 and

NoV2 3'Rz (Table 3). 2 μL of primer-extended cDNA was loaded into a PCR reaction for second-strand synthesis using Taq DNA Polymerase (Invitrogen) according to manufacturer's instructions. Thermal cycling parameters were 94°C x 2 min., 94°C x 30 sec., 55°C x 30 sec., 72°C x 4 min., then 29 cycles of 94 °C x 30 sec., 55 ° x 30sec., 72°C x 2min. The entire reaction was analyzed by gel electrophoresis on a 1% agarose gel, and the PCR product was excised from the gel and eluted with a MinElute Gel Extraction Kit (QIAGEN). Each product was subcloned into the pGEM-T Easy vector (Promega) and the resulting subclones were used to transform *E. coli* JM109cells (Promega). Transformants were selected for ampicillin resistance and for alpha-complementation (Figure 8) on 2xYT plates containing 100 mg/mL ampicillin, 0.01 mM Isopropyl β-D-1-thiogalactopyranoside and 0.26 mM X-Gal (Invitrogen).

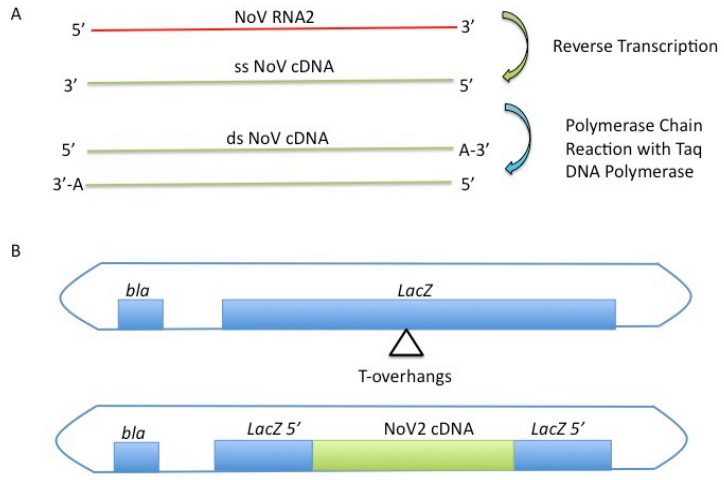

Figure 8: Screening of clonal isolates. A, Reverse transcription was performed on purified total cellular RNAs from BSRT7/5 cells transfected with plasmids containing NoV cDNAs (see Figure 9). This creates a ss cDNA that is complemented by PCR with Taq DNA polymerase and gene-specific oligonucleotide primers. Taq DNA polymerase adds a non-templated adenine onto the 3'-termini of PCR products approximately half the time, which allow its ligation into the TA cloning vector pGEM-T-Easy (**B**), The pGEM-T Easy vector contains single T overhangs at their 3' ends that base pair with the complementary overhanging A residues on the cDNA PCR product. These overhangs occur within the ORF of the *E. coli LacZ* the gene encoding β-galactosidase (β-gal), which cleaves the chromogenic substrate X-Gal to release a blue color. In transformed *E. coli*, cells that received a plasmid lacking a cDNA insert (top plasmid) express functional β-gal and cleave exogenously added X-Gal, resulting in a blue colony. The introduction of an insert interrupts the β-gal ORF so that cells transformed with a plasmid that contains an insert (bottom plasmid) will not express functional β-gal, resulting in a white colony. The *bla* gene encodes beta-lactamase and provides resistance to ampicillin for selection purposes.

Several white colonies were isolated and grown overnight in liquid cultures; plasmids were isolated and screened by cutting with *XbaI*, so that vectors in which the insert has been introduced generated fragments of 1358 and 3028 basepairs. Positive clonal isolates were subjected to DNA sequencing.

3.5 *In vitro* transcription and polyadenylation reactions

To generate *in vitro* transcripts of plasmids pNoV2 and pNoV2Δ3'10, plasmid DNA was linearized with *HindIII*, separated on a 1% agarose gel, and the linear form was isolated using with a Gel Extraction Kit (QIAGEN). *In vitro* transcription was performed with T7 RNA Polymerase (Promega) using 3.0 μg of linearized template DNA. Each reaction was treated with 1 μL of RQ1 DNase (Promega) for 20 minutes at 37°C. The resulting *in vitro* transcripts were purified using an RNeasy Mini Kit (QIAGEN) and eluted with 30 μL of DEPC-treated water (Ambion). For the *in vitro* polyadenylation assay, 0.5 μg of each RNA transcript was incubated in the presence or absence of 5 units of *E. coli* poly(A) polymerase (New England Biolabs) and 1 mM ATP per the manufacturer's recommendations. Reactions were incubated for 1 hour at 37°C, halted by the addition of 10x loading buffer (50% glycerol, 10mM EDTA, 0.25% bromophenol blue, 0.25% xylene cyanol FF), separated on a denaturing formaldehyde-agarose gel, and analyzed by Northern blot hybridization as described above.

CHAPTER 4

RESULTS

4.1 The 3'SL is a *cis*-acting RNA replication element in full length RNA2.

Our previous studies investigated the role of the 3'SL in RNA2 replication in plasmid-transformed cells of the budding yeast *Saccharomyces cerevisiae* (Rosskopf *et al.,* 2010). These studies used subgenomic RNA2-based replicons rather than full length NoV RNA2 and, while these and other replicons do replicate to reasonable levels in yeast and mammalian cells, they do so less well than does intact RNA2. This suggests that sequences elsewhere in RNA2 likely contribute to its replication. For example, in section 4.7 we describe a putative long-range interaction between the 3'SL loop and an upstream region in RNA2 that was removed from the replicons used previously (Figure 12). Therefore, for the purpose of the work described here, we used full-length RNA2 as the basis for all further mutagenesis. This may help us to identify additional *cis*-acting RNA replication signals required for optimal replication of RNA2.

In addition, we moved these studies from the yeast cells used by Rosskopf et al. (2010) to mammalian cells, which may be more physiologically relevant for NoV. Specifically, we used BSR-T7/5 cells, which are derivatives of baby hamster kidney BHK21 cells that constitutively express T7 RNA polymerase in the cytoplasm (Buchholz, 1997), the cellular compartment in which NoV replicates its genome (Ball and Johnson 1998). These cells direct synthesis of primary transcripts from plasmids containing genes of interest under transcriptional control of a bacteriophage T7 promoter. When these cells are transfected with plasmids that contain full-length cDNAs of NoV genomic RNA1 and RNA2 under transcriptional control of T7 promoters, the resulting primary transcripts

initiate a complete NoV replicative cycle *in vivo* (Figure 9), resulting in production of infectious virus (Johnson, *et al.* 2003). These cells were used for all of the studies described herein.

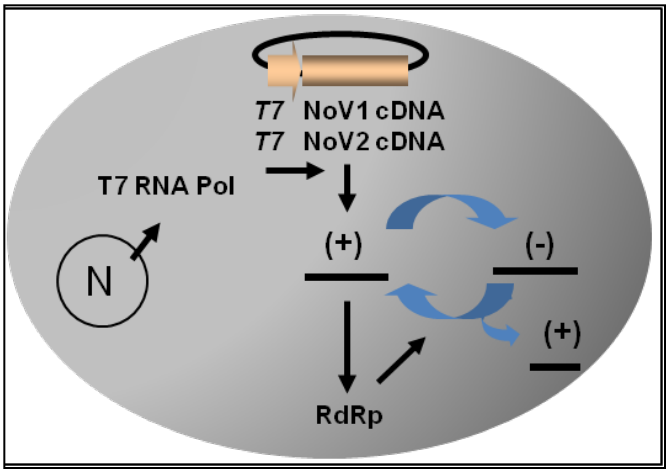

Figure 9: Launch of *Nodamura virus* replicative cycle in cultured mammalian cells. Mammalian BSRT7/5 cells are baby hamster kidney BHK21 cells constitutively expressing cytoplasmic bacteriophage T7 RNA polymerase (Buchholz, 1997). Upon transfection of plasmids pNoV1 and pNoV2, which contain full-length cDNA clones of NoV RNA1 and RNA2, respectively, under transcriptional control of T7 promoters (Johnson *et al.*, 2003), primary transcripts will be synthesized by T7 RNA polymerase. After their translation by the host machinery, they produce the NoV RdRp (and the capsid precursor proteins in the presence of RNA2). The RdRp can initiate active RNA replication of RNA1 and RNA2 (blue arrows), as indicated by the presence of negative strand genomic RNAs and both positive and negative strands of RNA3 (bottom right) (Johnson *et al.*, 2003). These events take place in the cytoplasm of transfected cells.

We first tested the effect of deleting the 3'SL on RNA2 replication. Therefore, the Δ3'SL mutant described by Rosskopf *et al.* (2010) was introduced into the full-length RNA2 cDNA clone, resulting in plasmid pNoV2-Δ3'SL. We transfected the WT or mutant versions of pNoV2 into BSR-T7/5 cells together with pNoV1 as a source of RdRp. Total cellular RNA was isolated and RNA2 replication products were analyzed by Northern blot hybridization using with probes specific for either the positive- or negative-strands of RNA2 (Rosskopf *et al.,* 2010). The positive strands were analyzed in Figure 10A and quantitated in Figure 10E, while the negative strands were analyzed in Figure 10B and quantitated in Figure 10F (monomers) and 10G (dimers)

The deletion of the 3'SL from RNA2 resulted in a severe defect in RNA replication in mammalian cells (Figure 10) that is similar to that described for the replicon

system in yeast (Rosskopf *et al.,* 2010). As shown in Figures 10F and 10G, the accumulation of monomeric negative strand RNA was reduced to 15% of the WT level, while synthesis of dimeric negative strand RNA2 was only reduced to 74% of WT (Figure 10G). Subsequent synthesis of monomeric positive strands was reduced to 18% relative to the WT level (Figure 10E).

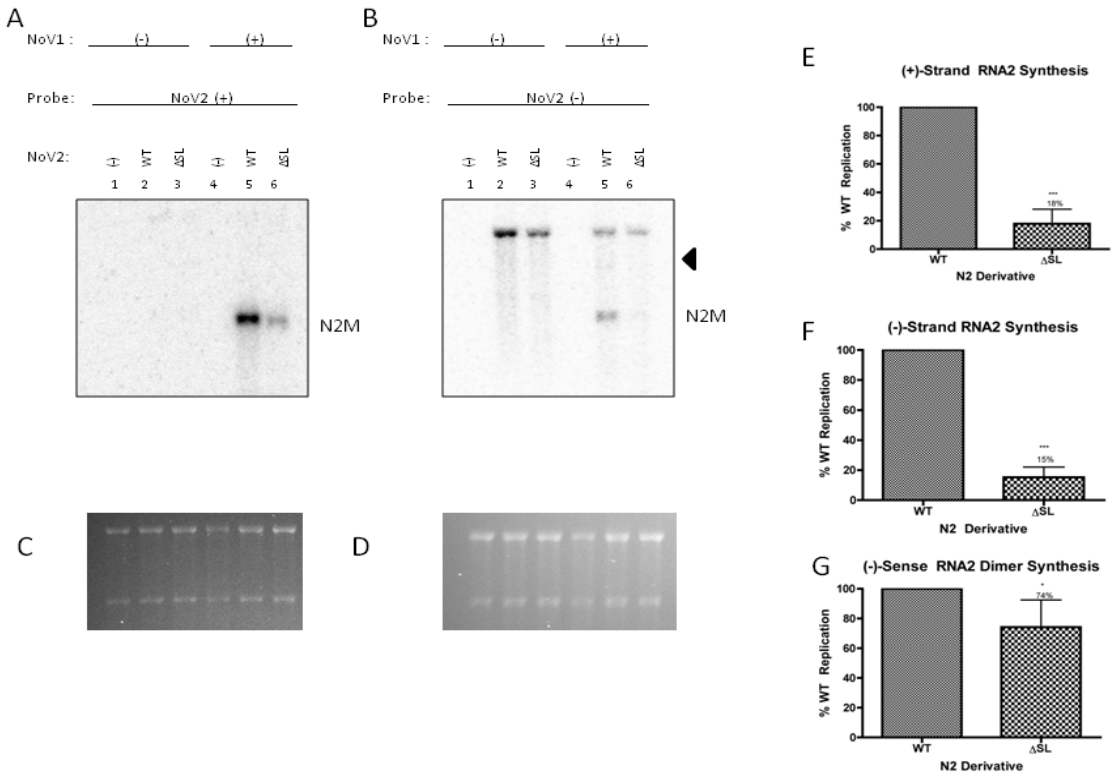

Figure 10: The 3'SL acts as a *cis*-acting RNA replication element in full-length RNA2. BSR-T7/5 cells were transfected with the indicated version of pNoV2 (WT vs mutant), together with pNoV1 as a source of RdRp. Total cellular RNA was isolated, separated on a denaturing formaldehyde-agarose gel, and transferred to charged Nylon membranes. RNA2 replication products were detected with ^{32}P-labeled riboprobes specific for the positive **(panel A)** or negative **(panel B)** strands of RNA2. The bold arrow represents dimeric RNA2 species, while monomeric RNA is indicated by N2M. Panels **C** and **D** show the cellular ribosomal RNAs (rRNAs) in the denaturing gels prior to transfer, as visualized by ethidium bromide staining, used to normalize the amount of RNA loaded in each lane. Panels E-G show quantitiave analysis of blots probed for the following RNA2 species: monomeric positive strands (**Panel E**), monomeric negative strands (**Panel F**), or dimeric negative strands (**Panel G**). Graphs indicate the mean of at least three independent experiments ± the standard deviation. Statistical analysis was conducted with a two-tailed paired-t test (α = 0.01).

These observations are in agreement with those of Rosskopf *et al.* (2010), where our laboratory reported that a chimeric RNA2-based replicon that lacked the 3'SL accumulated dimeric RNA2 at a level that was 71% of that detected for the WT replicon that contained the 3'SL. These data indicate that 3'SL does indeed play a role in RNA replication in full-length RNA2 in mammalian cells. We therefore asked which essential structural and sequence elements of the 3'SL were responsible for directing RNA replication by constructing two broad categories of mutations: those that affect the double-stranded stem and those that affect the single-stranded loop.

4.2 The structure of the 3'SL stem rather than its primary sequence is critical for RNA2 replication.

We tested the structural function of the stem by disrupting the base pairing interactions therein. Our first set of mutations was fairly conservative (Figure 11). We independently mutated the upstream side of the stem (nucleotides 1299-1305) from the WT 5'-GACCCUA-3' to the complementary sequence, 5'-CUGGGAU-3', yielding plasmid pNoV2-Up. Similarly, we mutated the downstream side of the stem (nucleotides 1316-1322) from WT 5'-UAGGGUC-3' to the complementary sequence, 5'-AUCCCAG-3', generating plasmid pNoV2-Down. Both of these mutations have the overall effect of making each side of the stem identical, which will preclude their ability to base pair, thereby disrupting stem formation. The final mutation in the set is a compensatory double mutation that restores base pairing by mutating both stems concurrently, with the net result of inverting the WT sequence of the stem (see Figure 11), generating plasmid pNoV2-Dbl. We tested the effect of these mutations on RNA replication by transfecting BSRT7/5 cells with either WT or mutant versions of RNA2, along with

pNoV1 as a source of RdRp, and analyzing them by Northern blot hybridization analysis as described above.

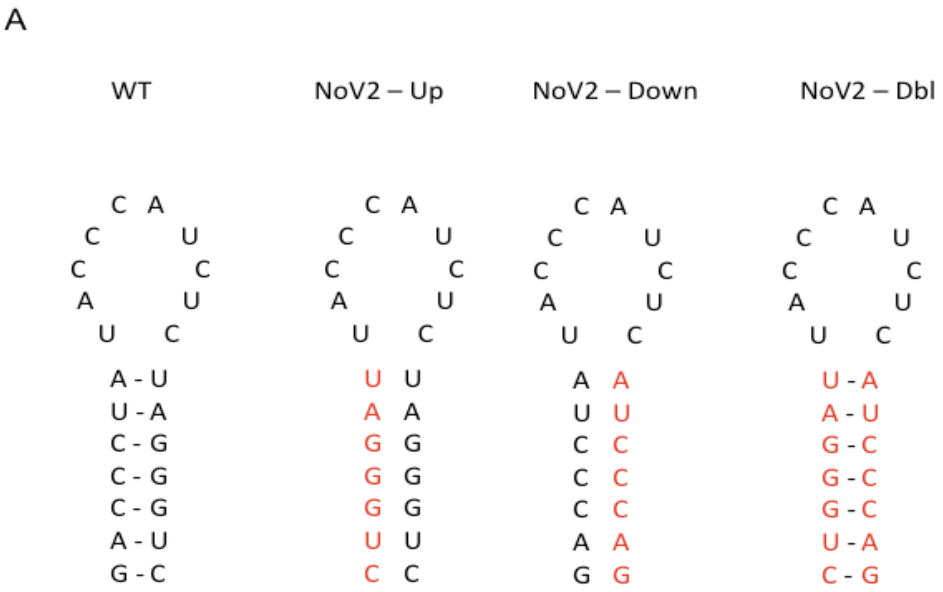

Figure 11: Conservative stem mutations. A, At left is shown the WT 3'SL. Site-directed mutagenesis was used to change all of the nucleotides on either the up- (NoV2-Up) or the downstream (NoV2-Down) side of the stem to the complementary nucleotide, predicted to interrupt base-pairing in the stem. The compensatory double mutation restored base pairing in the stem, essentially inverting the WT sequence.

The NoV2-Up mutation led to a decrease in accumulation of RNA2, with only 39% of WT levels of RNA2 negative strand monomers and 42% of the WT of negative strand dimers (Figure 12G). Subsequent positive strand synthesis was more severely affected, as the NoV2-Up mutant accumulated only 12% of the WT level of positive strand monomers (Figure 12E). Similarly, the NoV2-Down mutation directed accumulation of RNA2 negative strand monomers at 17% of the WT levels (Figure 12F) and negative strand dimers at 32% of WT (Figure 12G). Accumulation of positive strands was also reduced to 7% of the WT level (Figure 12E). For each mutation, the further reduction in positive strand synthesis suggests that perhaps the negative strand

RNA replication intermediates were not being used efficiently as templates for the synthesis of positive strands. Over the course of several experiments, the averaged value of NoV2-Down dimer synthesis was not significantly different than that of NoV2-Up but both were significantly reduced relative to WT. These data suggest that the base pairing in the 3'SL must play a role in synthesis of dimeric RNA2 negative strands, although the mechanism through which this occurs is unknown. The role of the negative strand dimers in RNA2 replication is unclear, although it has been suggested that they may serve as templates for positive strand synthesis (Albariño *et al*., 2001; Price *et al*., 2005; Rosskopf *et al*., 2010).

As hypothesized, the NoV2-Dbl mutation that restores base pairing in the stem, rescued synthesis of both positive- and negative-strand RNA to near WT levels (Figures 12E and 12F, respectively); the slight decrease we detected in monomeric negative strand synthesis (73% of WT levels) was not statistically significant (Figure 12F). These results suggest that base pairing in the 3'SL stem is indeed a requirement for RNA2 replication. The restoration of dimer synthesis to near-WT levels (76% of WT) suggests a correlation between synthesis of the negative strand RNA2 dimers and monomeric positive strands (Figure 12G), as suggested above and previously by Rosskopf *et al.* (2010).

While the previous mutations demonstrate the necessity for base pairing in the stem, it remained possible that the primary sequence of the stem played some role in this process, since the compensatory NoV2-Dbl mutation restored base pairing but had the net result of inverting the WT stem sequence. We were concerned that this mutation might not preclude sequence-specific RNA-protein interactions, resulting in near WT

levels of RNA replication. Therefore, our next set of mutations more radically altered the stem by introducing non-WT sequences into the stem.

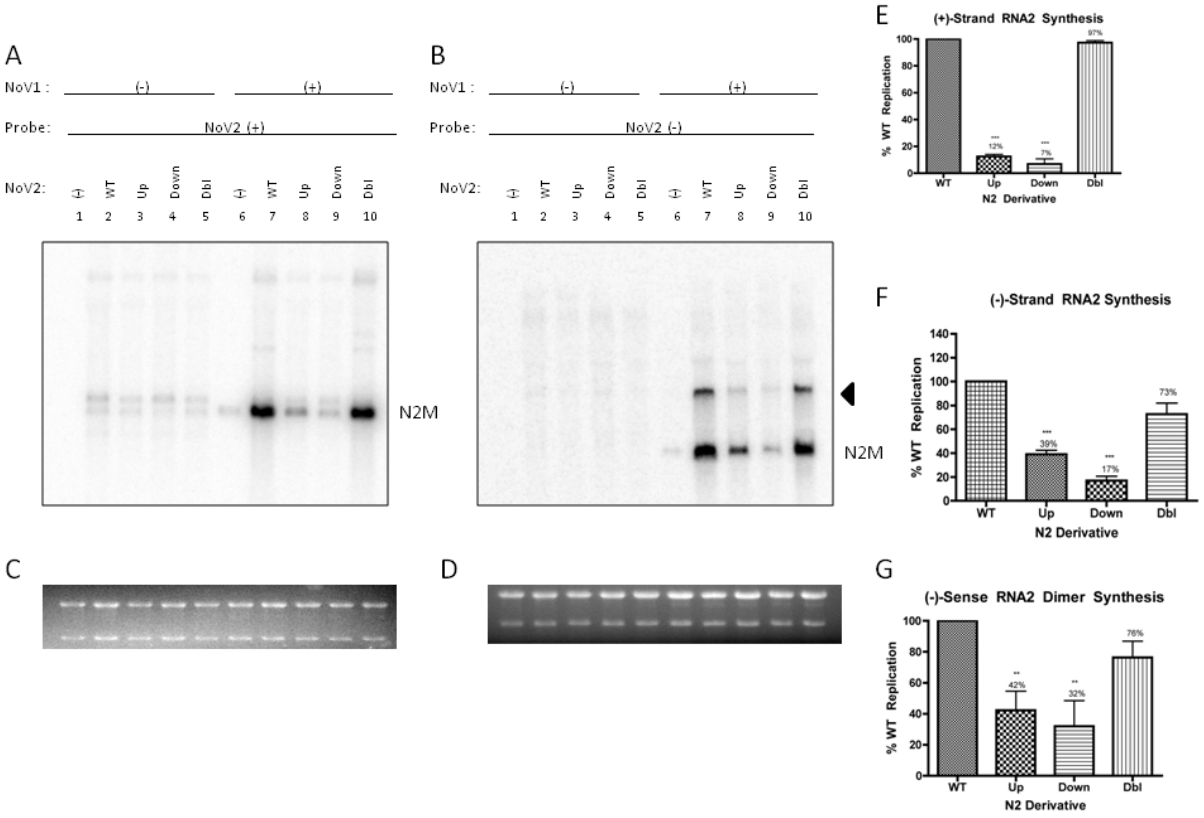

Figure 12. Base pairing in the stem rather than the primary nucleotide sequence is essential for RNA2 replication. Covariation mutagenesis present in the NoV2-Dbl construct mutated both stems concurrently, restoring base-pairing with the net result of inverting the WT sequence. Below are shown two representative Northern blots probing total cellular RNA for the presence of either the positive or negative strand of RNA2 (**A** and **B**, respectively). The bold arrow represents dimeric RNA2 species, while monomeric species are indicated by N2M. **C** and **D**, images of the ethidium bromide-stained ribosomal RNAs taken immediately after electrophoresis and before transfer, used to normalize the amount of RNA loaded per lane. Quantitiave analysis of blots probing for monomeric positive-strand RNA2 (**E**), monomeric negative strand RNA2 (**F**) and dimeric negative strand RNA2 (**G**) species are shown. Graphs indicate the mean of independent experiments and the standard deviation. Statistical analysis was conducted with one-way ANOVA and a Tukey's range post test (α = 0.01).

4.3 Restoration of base pairing in the stem with a different sequence also restored WT levels of RNA2 replication.

We introduced transversion mutations into each stem (Figure 13): all purines were changed to pyrimidines and vice versa, resulting in A-to-C, C-to-A, G-to-U, and U-to G substitutions. Thus, the NoV2-S1T mutation altered nucleotides 1299-1305 on the upstream side of the stem to 5'-UCAAAGC-3', while the NoV2-S2T mutation replaced nucleotides 1316-1322 on the downstream side of the stem with the sequence 5'-GCUUUGA-3'. Both mutations disrupted base pairing in the stem. The compensatory double NoV2-DST (*d*ouble *s*tem *t*ransversion) mutation replaces the WT nucleotides on both sides of the stem with transverse sequences, and putatively restores base pairing.

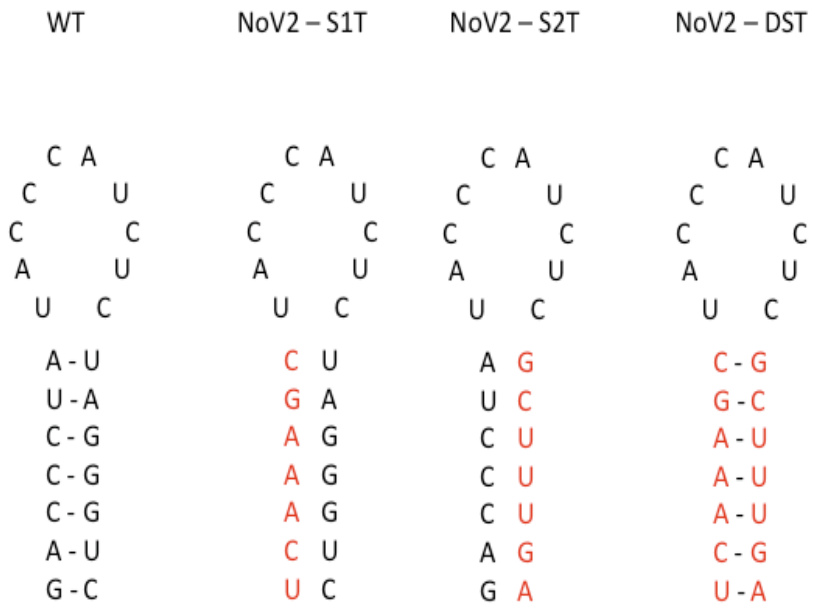

Figure 13: More radical stem mutations. Shown are schematic representations of mutations in which adenosine and cytosine residues are switched, as are guanosine and uridine residues, in either the upstream (NoV2-S1T) or downstream (NoV2-S2T) stem, or both stems concurrently (NoV2-DST).

As predicted by the phenotype of the NoV2-Up mutant, the NoV2-S1T mutation led to a decrease in accumulation of negative strand RNA2 monomers (Figure 14F),

which were 37% of WT levels. Interestingly, although accumulation of negative strand dimers was reduced to 49% of the WT levels, further analysis suggested that this reduction was not statistically significant (Figure 14G), largely due to fluctuation in RNA2 levels from one experiment to another. Indeed, the average level of NoV2-S1T dimer synthesis (49%) was close in value to those synthesized by NoV2-Up (42%). As with NoV2-Up, we also observed a reduction in accumulation of RNA2positive strands, to 19% of WT levels, as would be expected by the reduction in negative-strand synthesis (Figure 14E).

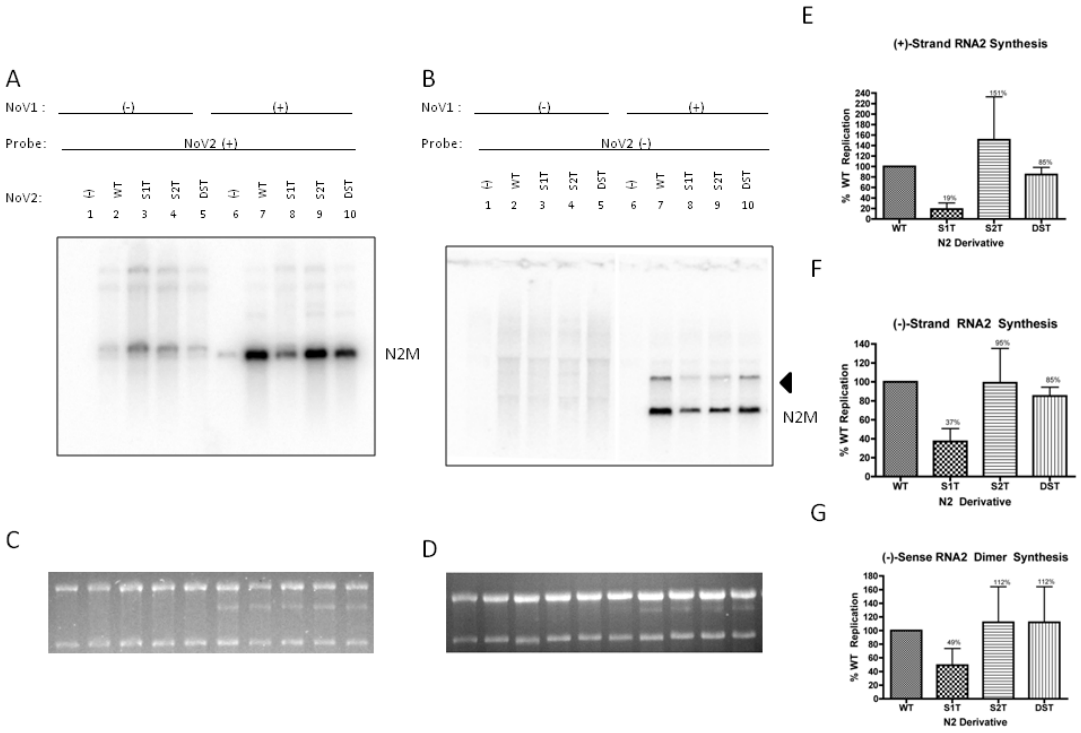

Figure 14: Restoration of base pairing in the stem with a different sequence also restored WT levels of RNA2 synthesis. Transversion mutations in 3'SL changed the stem sequence more radically. Shown are two representative Northern blots probing total cellular RNA for the presence of either the positive- or negative- strands of RNA2 (**A** and **B**, respectively). The bold arrows denote dimeric RNA2, while monomeric species are designated N2M. **C** and **D**, as before, ethidium bromide-stained ribosomal RNAs were as RNA loading controls. Quantitative analysis of blots probed for monomeric positive strand RNA2 (**E**), monomeric negative strand RNA2 (**F**) and dimeric negative strand RNA2 (**G**) species are shown. Graphs indicate the mean of independent experiments and the standard deviation. Statistical analysis was conducted with one-way ANOVA and a Tukey's range posttest (α = 0.01).

Surprisingly the behavior of the NoV2-S2T mutant in transfected mammalian cells was completely different than predicted by that of the analogous NoV2-Down mutant. This mutation did not abrogate RNA2 accumulation as predicted: the average amount of monomeric negative-strand RNA2 accumulation over the course of five experiments was 95% of WT levels, with several experiments indicating higher-than-WT RNA2 accumulation (Figure 14F). Negative strand RNA2 dimers also accumulated at a mean 112% of WT (Figure 14G). Over the course of the same five experiments, we observed accumulation of positive strands at 151% of WT levels (Figure 14E), suggesting that these negative strands were efficient templates for positive strand synthesis.

We were initially puzzled by this result since this mutation was expected to disrupt base paring in the stem as had NoV2-Down and NoV2-S1T. We therefore subjected the entire NoV2-S2T segment to structure prediction analysis. The mfold program (Zuker, 2003) predicted that the most thermodynamically favorable full-length RNA2-S2T RNA molecule is 8.50 kcal/mol less stable than full-length WT RNA2 (Table 1). When we folded the 3'-terminal 100 nucleotides of NoV2-S2T with PseudoknotsRG (Reeder and Giegerich, 2004), we could confirm that the WT stem was indeed disrupted (Figure 15).

However, this region was predicted to form an alternative stem loop structure with a 10-nucleotide stem (nucleotides 1256-1263 base paired with nucleotides 1315-1322), internal bulging of nucleotides 1264 and 1312-1314, and a second stem in which nucleotides 1265 and 1266 base paired with nucleotides 1310 and 1311 (Figure 15).

The loop structure consisted of 46 nucleotides (1267-1309) and was predicted to include two smaller stem loops.

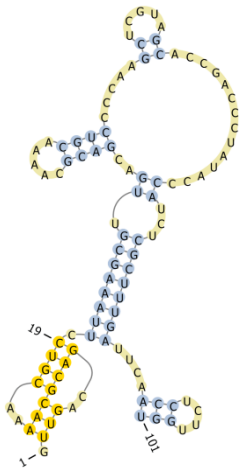

Figure 15: A predicted alternative structure in the NoV2-S2T RNA. The 3'-terminal nucleotides of RNA2 were folded with PseudoknotsRG (Reeder & Giegerich, 2004). Substituting the WT sequence of the 3' stem is predicted to alter the architecture of the 3'SL. Interesting, nucleotides 1316-1322 are predicted to remain double-stranded, similar to the WT structure, albeit with different basepairing partners. This structure may serve as a functional alternative to the WT SL to promote RNA replication.

We hypothesize that this alternative structure may form a preferential template for synthesis of negative strand RNA2 monomers and dimers as compared to the WT 3'SL structure, leading to robust accumulation of monomeric RNA2 positive strands (Figure 15).

Despite the anomalous behavior of NoV2-S2T, the NoV2-S1T mutation clearly disrupted base pairing in the 3'SL stem and adversely affected accumulation of RNA2, as expected. Therefore, we constructed the corresponding double transversion mutant, NoV2-DST, with the intention of restoring base pairing in the stem with a sequence that is different from that of WT or the NoV2-Dbl mutant. The compensatory NoV2-DST mutation, which is predicted to form a 3'SL in the same position as WT RNA2 (Figure 16), rescued the accumulation of RNA2 species lost by NoV2-S1T.

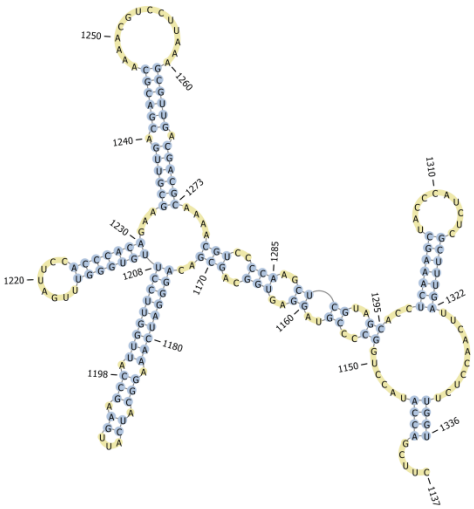

Figure 16: A compensatory double mutation with non-WT sequences is predicted to allow 3'SL structure formation. The 3'-terminal 200 nucleotides of RNA2 were folded with PseudoknotsRG (Reeder and Giegerich, 2004) and imaged with Pseudoviewer. Note how the 3'SL retains WT-positioning, as it is still 14 nucleotides from the 3'-terminus.

The accumulation of negative strand RNA2 monomers and dimers was also restored to near WT levels, with 85% of WT levels of monomers (Figure 14F) and 112% of WT levels of dimers (Figure 14G). Correspondingly, positive strand accumulation was 85% of WT levels (Figure 14E). For both positive and negative strand RNA2 species, these slight decreases in RNA2 accumulation were not statistically significant. These data suggest that the 3'SL functioned even with an altered stem sequence.

Taken together, these results indicate that base pairing in the stem is a requirement for regulating synthesis of negative strand monomers and dimers and positive strands monomers of NoV RNA2. However, while the six mutations considered in this section examined the role of base pairing and primary sequence in the 3'SL stem, they all contained the WT seven base pairs in the stem. We therefore wondered whether the length of the stem is also important for RNA2 replication.

4.4 A shortened 3'SL stem does not support WT levels of RNA2 accumulation.

We examined the effect of altering the 3'SL stem size on RNA replication by deleting the internal three G-C base pairs of the WT stem (Figure 17). The NoV2-ΔSBP mutation generates a 3'SL element that lacks three *s*tem *b*ase-*p*airs. The upstream side of the resulting shortened stem has the sequence 5'-GAUA-3' while the downstream side has the sequence 5'-UAUC-3'.

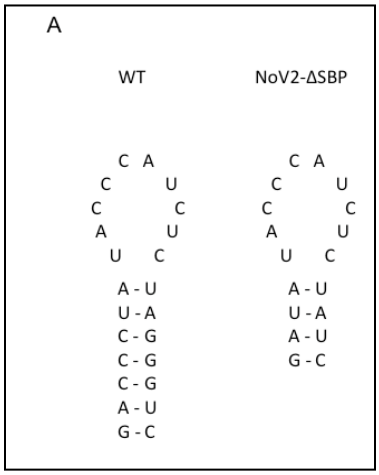

Figure 17: A shortened stem sequence that deletes three internal C—G basepairs. Deleting the three internal basepairs is predicted to leave a four-basepair stem.

When the resulting NoV2-ΔSBP plasmid was transfected into BSR-T7/5 cells, we observed a severe defect in RNA2 replication. We detected only 18% of WT levels of negative strand monomers (Figure 18F) and 62% of the WT level of dimers (Figure 18G). Similarly, we detected only 11% of WT levels of positive strands (Figure 18F).

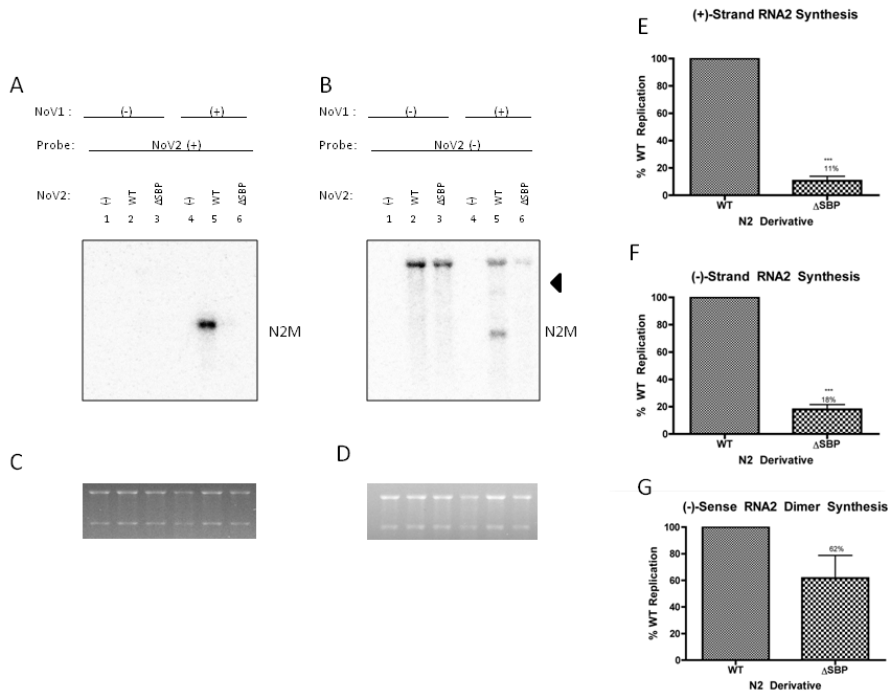

Figure 18: A shortened stem sequence cannot support WT levels of RNA2 synthesis. Three internal G—C basepairs were deleted from the WT SL, resulting in a four basepair stem. Shown are two representative Northern blots probing total cellular RNA for the presence of either the positive or negative strand of RNA2 (**A** and **B**, respectively). The bold arrow represents dimeric RNA2 species, while monomeric species are indicated by N2M. **C** and **D**, images of the ethidium bromide-stained ribosomal RNAs taken immediately after electrophoresis and before transfer, used to normalize the amount of RNA loaded per lane. Quantitiave analysis of blots probing for monomeric positive strand RNA2 (**E**), monomeric negative strand RNA2 (**F**) and dimeric negative strand RNA2 (**G**) species are shown. Graphs indicate the mean of independent experiments and the standard deviation. Statistical analysis was conducted with one-way ANOVA and a Tukey's range post test (α = 0.01).

These data might be interpreted as suggesting that the length of the 3'SL stem plays a direct role in RNA2 replication. However, we consider it more likely that the shortened 3'SL element may lack the structural integrity possessed by the WT structure. Indeed, if these sequences were not sufficient for formation of a 3'SL structure, one would expect to see a severe decrease in RNA replication, as is suggested by our

previous mutations. The NoV2-ΔSBP mutant 3'SL structure, an 18-mer, is projected to have a ΔG of -0.50 kcal/mol, which is in turn a change in ΔG of 7.90 kcal/mol from the WT 24-mer (Table 1).

This instability could destabilize the loop to such an extent that structure formation of the 3'SL is inhibited. Indeed, the ten nucleotides of the loop could serve as a destabilizing force, leading to unwinding of the weaker four-member stem and thereby disrupting formation of the 3'SL completely. Indeed the phenotype of this mutant is reminiscent of that exhibited by the deletion mutant (Figure 10).

Clearly, the 3'SL structure must retain exacting requirements for coordinating the activities in which it participates (e.g. synthesis of both dimers and monomers of RNA2). Point mutation analysis would aid in determining whether insertion or deletion of single nucleotides or base pairs into the stem would also affect RNA replication. The results obtained with this mutation reinforce our previous conclusions that the structural integrity of the stem is important for RNA2 replication.

4.5 The 3'SL plays a role in synthesis of both polarities of RNA2.

As noted above, the 3'SL forms near the 3' end of the RNA2 positive strand, yet mutating it affects synthesis of both positive and negative strands. Since an analogous structure is predicted to form near the 5' end of the negative strand (data not shown), we wondered whether both polarities were required for RNA2 replication. The mutations described so far have shown no strand specificity, i.e., any of them could function in the negative as well as (or instead of) in the positive polarity. We therefore constructed

mutations in which the 3'SL can form in only the positive or only the negative strand (Figure 19).

Our strategy for constructing these polarity mutations takes advantage of the ability of RNA molecules to form G-U base pairs. If we envision a double-stranded stem in the positive strand, a C on one side of the stem can base pair with a G on the other. If that C is changed to a U, it can still base pair with the same G and the stem will be unaffected in the positive strand. However, when the positive strand U and G in question are transcribed into the complementary negative strand, these nucleotides will become A and C, which will no longer base pair in the negative strand. A similar strategy can be used to generate a mutation that affects base pairing in the positive strand but not in the negative.

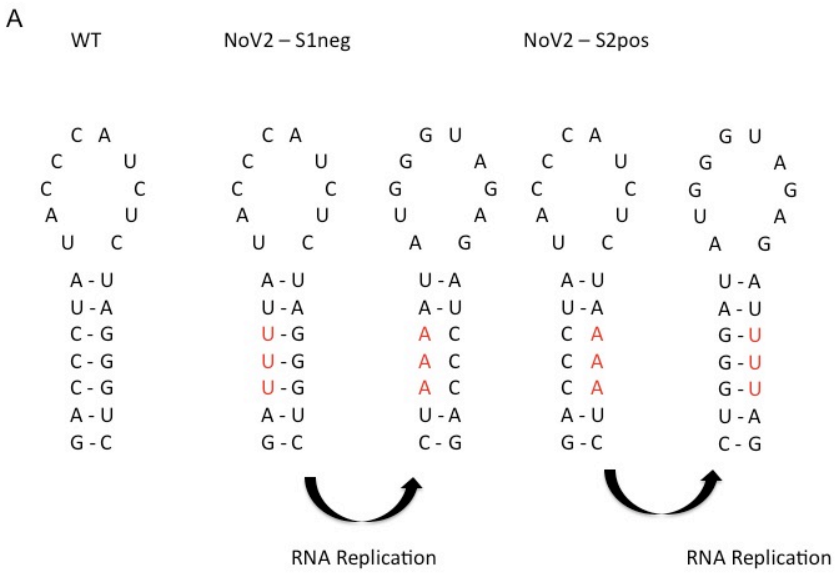

Figure 19: Mutations that affect 3'SL stem formation in a strand-specific manner. Shown at left is the WT 3'SL sequence. When the three C's on the upstream site of the stem are replaced with U's (center, NoV2-S1neg), G-U base pairing allows the stem to form in the positive strand, but upon copying into the negative strand, stem formation is precluded by A-C mismatches. Conversely, when the three G's on the downstream site of the stem are replaced with A's (right, NoV2-S2pos), the stem is no longer able to form in the positive strand but again G-U base pairing allows the stem to form in the negative strand.

Using this approach, we constructed NoV2-S1neg, which alters the upstream side of the stem from the WT 5'-GACCCUA-3' to 5'-GAUUUUA-3' (Figure 20). In this

case, the 3'SL could still form with a U-G base pair in the positive strand but its formation would be precluded in the negative strand by an A-C mismatch. Conversely, NoV2-S2pos alters the downstream side of the stem from WT 5'-UAGGGUC-3' to 5'-UAAAAUC-3', thereby disrupting base-pairing in the positive strand with a C-A mismatch, but forming a G-U base pair in the negative strand (Figure 19).

As before, we tested the ability of the resulting mutants to replicate in BSR-T7/5 cells when co-transfected with pNoV1 as a source of RdRp. The NoV2-S1neg mutant, in which the stem can form only in the positive strand, exhibited a significant decrease in accumulation of both positive and negative strands. We detected an average of 36% of WT levels of positive strand RNA2 (Figure 20E), 34% of WT levels of negative strand monomers RNA2 (Figure 20F), and 75% of WT levels of negative strand dimers (Figure 20G). Interestingly, this mutation resulted in near-equimolar (1:1) accumulation of positive and negative strands (compare Figure 21E with 21F). This contrasts with the 100:1 positive-to-negative strand ratio observed for WT RNA2 (Ball *et al.*, 1992; Johnson *et al.*, 2003), suggesting that 3'SL may play a role in coordination of positive and negative strand synthesis.

Similarly, the NoV2-S2pos mutant, in which the 3'SL is unable to form in the positive strand but is able to form in the negative strand, exhibited a defect in RNA2 replication. For this mutant, we detected 27% of WT levels of positive strands (Figure 20E), accumulation of negative strand monomers at 40% of WT (Figure 20F), and negative strand dimers at 74% of WT levels (Figure 20G). It is interesting to note that with both of these mutations, the polarity of the RNA in which the 3'SL could still form was observed to accumulate to higher levels than the counterpart RNA.

Taken together, these data indicate that the 3'SL functions in both polarities of the RNA. In the positive strand, the 3'SL may serve as an initiation site for the synthesis of negative strand RNA replication intermediates. In the negative strand RNA, the 3'SL may function in an alternative manner, perhaps in coordinating template selection or positive strand initiation from a negative strand template. These possibilities are considered further in the Discussion.

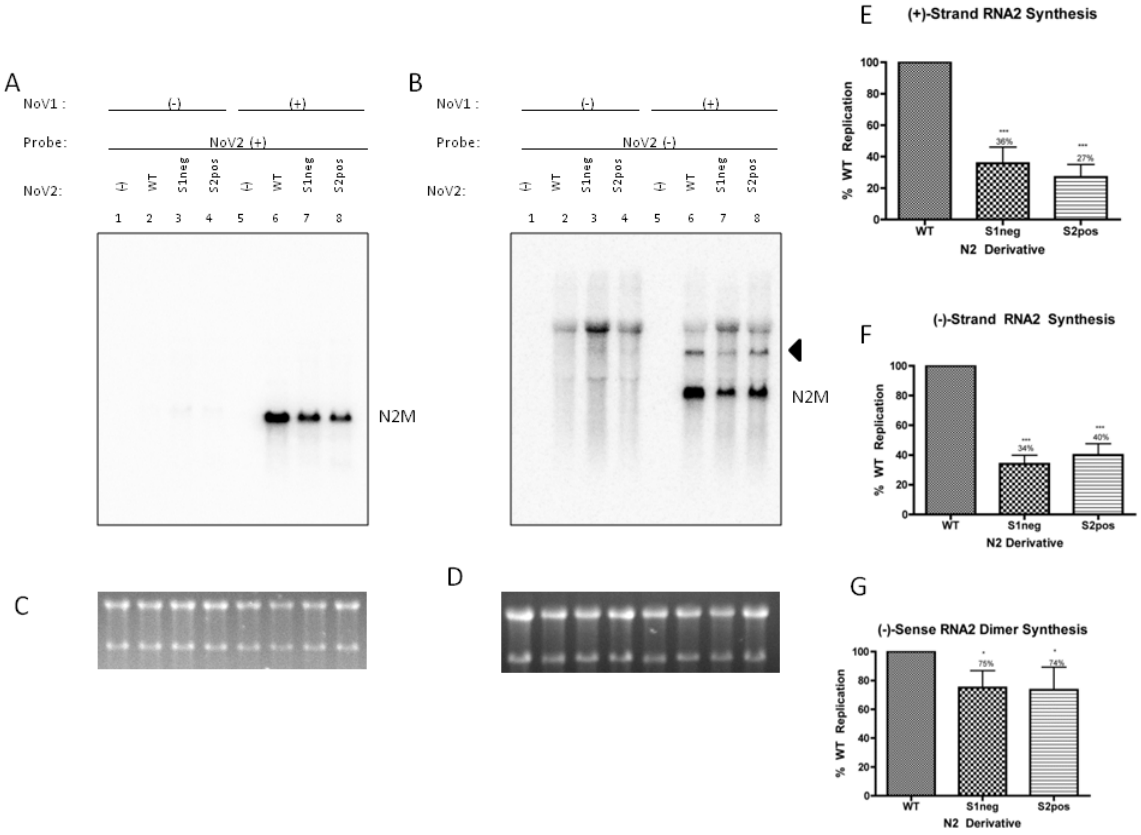

Figure 20: The 3'SL must form in both the positive and negative strands for full RNA2 replication. Shown are two representative Northern blots in which total cellular RNA was probed for the presence of either the positive or the negative strand of RNA2 (**A** and **B**, respectively). The bold arrow represents dimeric RNA2 species, while monomeric species are indicated by N2M. **C** and **D**, images of the ethidium bromide-stained ribosomal RNAs taken immediately after electrophoresis and before transfer, used to normalize the amount of RNA loaded per lane. Quantitiave analysis of accumulation of positive strand (**E**), monomeric negative strands (**F**), and dimeric negative strands (**G**) is shown. Graphs indicate the mean of independent experiments and the standard deviation. Statistical analysis was conducted with one-way ANOVA and a Tukey's range posttest (α = 0.01).

These stem mutations have given us valuable insight into the structural and sequence requirements of the 3'SL stem in RNA replication. Considered together, we conclude that the primary sequence of the stem region is not particularly important but that its secondary structure is critical for RNA2 replication. Additionally, the 3'SL must form in both strands of the RNA for optimal RNA2 replication. If the stem structure is so critical, we wondered what, if any, role in RNA2 replication is played by the single-stranded 3'SL loop.

4.6 3'SL loop sequence and structure remain critical for directing RNA replication.

We next investigated which components of the single-stranded loop might be important for RNA2 replication. We considered both loop size and sequence with a series of mutations (Figure 21). The first mutation, NoV2-TransLoop (TL), altered the WT loop sequence from 5'-UACCCAUCUC-3' to 5'-GCAAACGAGA-3'. Because this mutation contains the same number of single-stranded nucleotides as the WT loop, we also constructed a series of mutations in which the loop was reduced in size. First, we created a tetraloop with the sequence 5'-GAGA-3'. Tetraloops are thermodynamically favorable structures, as four bases is the optimum size to span a double-stranded helix of RNA (Antao *et al.*, 1991). Indeed, mfold analysis indicates that this 18-mer is -3.20 kcal/mol more stable than the WT 24-mer (Table 1). We also created a triloop with the sequence 5'-UCA-'3. This structure was indeed still predicted to be thermodynamically favorable when analyzed with mfold, as the predicted ΔG of this 17-mer is -0.50 kcal/mol more stable than the WT SL (Table 1). We then asked whether deleting all ten nucleotides of the WT loop would affect RNA replication. Realistically, the structure as depicted in Figure 21 is unlikely to actually form; analysis with mfold suggests that the

two A-U base pairs at the top of the stem would be disrupted in the absence of the loop, as depicted by the lack of hydrogen bonds between these base pairs in Figure 21, leading to a small, single-stranded tetraloop and a shortened stem. However, this mutant will indicate whether deleting the ten nucleotides from the WT loop is deleterious to RNA2 replication. An interesting side effect of these mutations is that they allowed us to examine the effect of loop stability as well as primary sequence and size with these mutations.

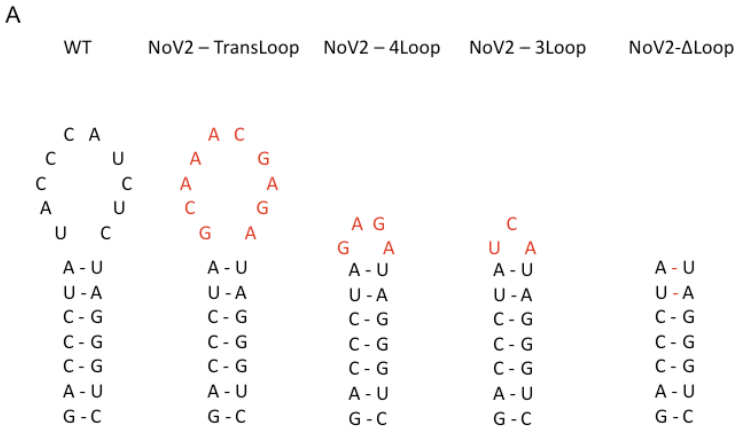

Figure 21: Loop mutations for testing the role of the 3'SL loop sequence and structure in RNA2 replication. The mutations shown replace the 3'SL loop with a transverse sequence (TransLoop) or decrease its size from the WT ten bases to either four bases (4Loop), three bases (3Loop) or no bases (ΔLoop).

We first tested the effect of mutating the single-stranded nucleotides of the 3'SL loop sequence using the transversion mutation scheme (NoV2-TransLoop) described earlier. We detected only 55% of WT-levels of positive strand accumulation (Figure 22E) and 52% of negative strands (Figure 22F). Synthesis of negative strand dimers was reduced to 43% relative to WT (Figure 22G). NoV2-LT synthesized positive strand RNA2 at a level approximately four-fold higher than NoV2-Up and almost eight-fold higher than NoV2-Down, but remarkably, NoV2-LT synthesized approximately the same amount of negative strand dimers as these mutants (42% and 32%, respectively). It is

possible that the sequence present in the loop may interact with other sequences throughout the RNA molecule to promote RNA replication.

We tested the effect of engineering a stable tetraloop structure at the top of the stem. This mutation synthesized only 41% of WT levels of positive strand RNA2 (Figure 22E) and 47% of WT negative strand RNA2 levels (Figure 22F). These data are in agreement with our hypothesis that further structure and sequence rearrangement of the loop is progressively more detrimental towards directing RNA replication. Synthesis of negative strand dimers was similarly impacted, as NoV2-4Loop synthesized only 30% of WT levels of dimeric RNA2 (Figure 22G).

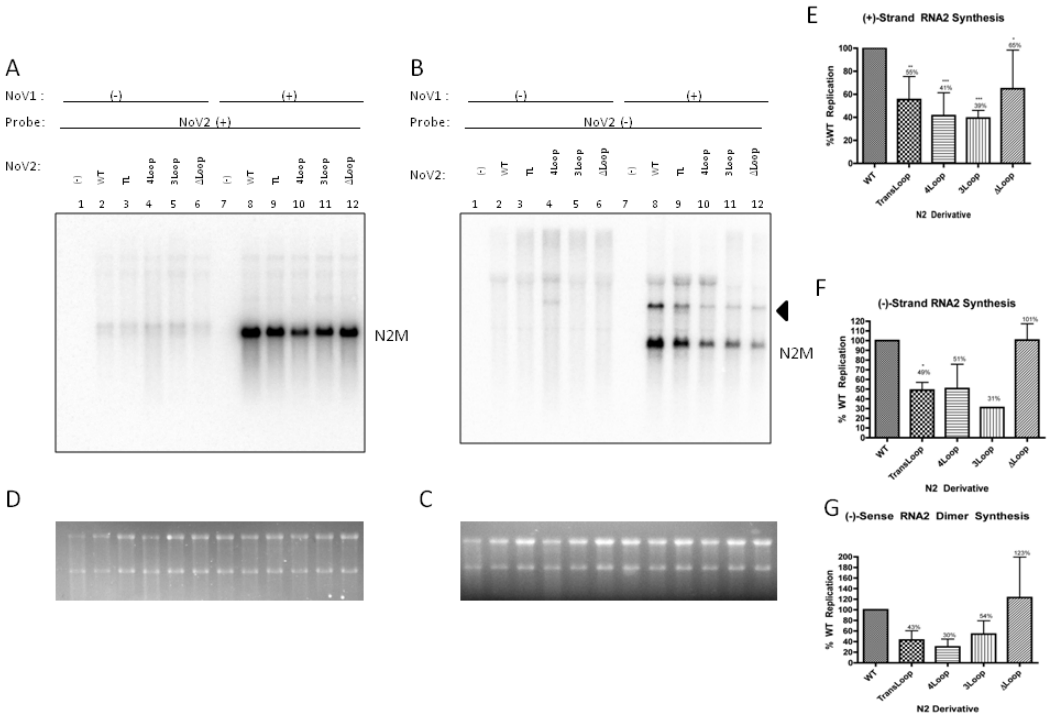

Figure 22: Loop size and sequence are important for coordinating RNA2 replication. Shown are two representative Northern blots probing total cellular RNA for the presence of either the positive or negative strand of RNA2 (**A** and **B**, respectively). Bold arrow, dimeric RNA2 species; N2M, monomeric RNA2 **C** and **D**, ethidium bromide-stained ribosomal RNAs, used as loading controls. Quantitiave analysis of blots probing for monomeric positive strand RNA2 (**E**), monomeric negative strand RNA2 (**F**) and dimeric negative strand RNA2 (**G**) species are shown. Graphs indicate the mean of independent experiments and the standard deviation. Statistical analysis was conducted with one-way ANOVA and a Tukey's range post test (α = 0.01).

To further test the size limitations of the 3'SL loop, we inserted the randomly generated sequence 5'-UCA-3' onto the WT stem, creating NoV2-TriLoop ("3Loop"). As hypothesized, this mutation similarly affected positive strand RNA2 accumulation, as we detected only 39% of WT levels (Figure 22E). The unfortunately poor quality of several replicates of this experiment allowed us to quantitate only a single blot, which indicated that the NoV2-3Loop construct replicated negative strand RNA2 31% relative to WT. Further replicates are planned for the future to confirm these results.

Synthesis of negative strand dimers was 54% relative to WT (Figure 22H), a slight increase over NoV2-4Loop and NoV2-3Loop. It is interesting that the correlation between decreasing loop size and loss of dimer accumulation was reversed. We had initially hypothesized that a four-member loop might represent a basal element for directing RNA replication, and that further deletion would abrogate RNA2 replication, yet the observation that NoV2-3Loop synthesized on average 24% MORE dimeric negative strand RNA2 than NoV2-4Loop intrigued us. We therefore altered our hypothesis to propose that a full deletion of the loop would result in synthesis of a similar amount of monomeric positive strand RNA as made by NoV2-3Loop and NoV2-4Loop, but more dimeric negative strand RNA2.

We tested this hypothesis with a complete deletion of the loop, NoV2-ΔLoop, resulting in a "bald" stem (Figure 21). To our surprise, this mutant averaged 65% of WT-levels of positive strand RNA2 accumulation over the course of eight experiments: 24% more than NoV2-4Loop and 26% more than NoV2-3Loop (Figure 22E). Correspondingly, we detected 90% of WT-levels of negative strand RNA synthesis, almost double the amount synthesized by NoV2-4Loop and near three-fold higher than

that of the NoV2-3Loop replicate (Figure 22F). Synthesis of the negative strand dimmer was on average 123% of WT (Figure 22G), a surprising observation considering the magnitude of this increase. Considering all of the loop mutations we have tested to date, we conclude that both the primary sequence of the loop and the number of single-stranded bases present in the loop influence RNA2 replication levels.

As mentioned, an advantage of utilizing full-length RNA2 in this work is that it allows us to investigate whether predicted long-range structural interactions between the 3'SL and sequences elsewhere in the RNA affect RNA replication. Since, as noted above, both the primary loop sequence and the size of the loop play important roles in RNA2 replication, we concluded that the nucleotides in the loop may be participating in RNA-RNA interactions or RNA-protein interactions, or both. We therefore set out to determine whether previously predicted long range interactions between the 3'SL loop and a region upstream (Johnson and Leung, unpublished data; Figure 23), were also important for RNA2 replication.

4.7 An upstream hexanucleotide sequence predicted to be involved in a long-range interaction with the 3'SL is implicated in RNA2 replication

Preliminary data from our lab suggest that nucleotides in the loop region of the 3' stem loop might be involved in a long-range interaction (LRI) with nucleotides approximately 650 base pairs upstream (Figure 23). The PseudoKnotsRG software predicts that nucleotides 1309-1314 of the 3' stem loop may base pair with nucleotides 660-656, respectively. Our collaborator, Dr. Ming-Ying Leung (a Professor in UTEP's Department of Mathematical Sciences and Director of the Bioinformatics Graduate

Program) predicted that the adenosine at position 655 in RNA2 might also participate in this interaction, base pairing with the corresponding uracil in the 3'SL loop (Leung, personal communication). This prediction supports our previous argument that a sequence elsewhere in the RNA molecule may act as a RBP binding site and aid in positioning the RdRp near the 3'-terminus of genome for RNA replication, and we therefore targeted this sequence for further study.

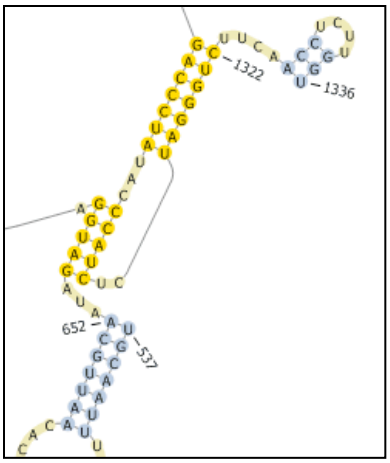

Figure 23: A putative long-range interaction may form in NoV RNA2. Depicted is the potential long-range interaction between nucleotides in the NoV RNA2 3'SL (nt 1309-1314) and a region approximately 650 nucleotides upstream (nt 655-660). The 3'-terminal 800 nucleotides of RNA2 were folded with PseudoknotsRG and viewed with Pseudoviewer3.0. Shown at the bottom is the distal sequence with the participating nucleotides shown in yellow.

We tested this hypothesis through mutagenic analysis of both the upstream region (UR) and the nucleotides in the loop (Figure 24). We first started by deleting nucleotides in the UR, resulting in plasmids pNoV2-Δ655 (deleting nucleotides 655-660) and pNoV2-Δ656 (deleting nucleotides 656-660), and assaying the relative amounts of RNA2 accumulation. Secondly, to interrupt the putative long-range basepairing interaction between these two elements, we introduced transverse sequences into the UR similar to our experiments with the stems and loop of the 3' stem loop, such that the WT sequence 5'-AGAUGG-3' is replaced with 5'-CUCGAA-3', generating the construct pNoV2-655T. Lastly, in conjunction with the aforementioned 'loop transversion' mutation, we will again mutate the UR with a complementary transverse sequence, thus restoring the potential interactions in the pseudoknot via plasmid pNoV2-MLRI (Figure 24).

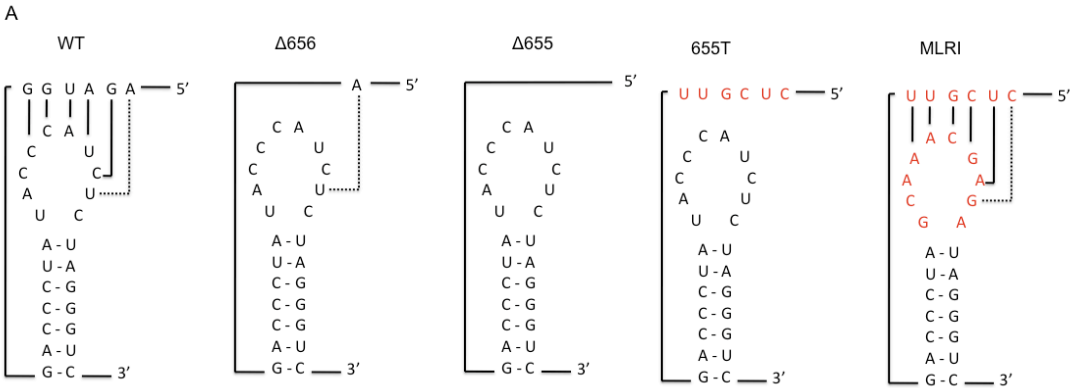

Figure 24: Mutations designed to test the role of the putative pseudoknot in RNA replication. A, Shown at left is the predicted interaction occurring in WT RNA2. Deleting nucleotides 656-660 (Δ656) or nucleotides 655-660 (Δ655) will potentially abrogate pseudoknot formation. Similarly, substituting the upstream nucleotides with a transverse sequence (655T) will also affect structure formation. Using covariation mutagenesis, we will mutate the SL and the upstream region concurrently, with the hypothesis that this will allow for basepairing to be restored

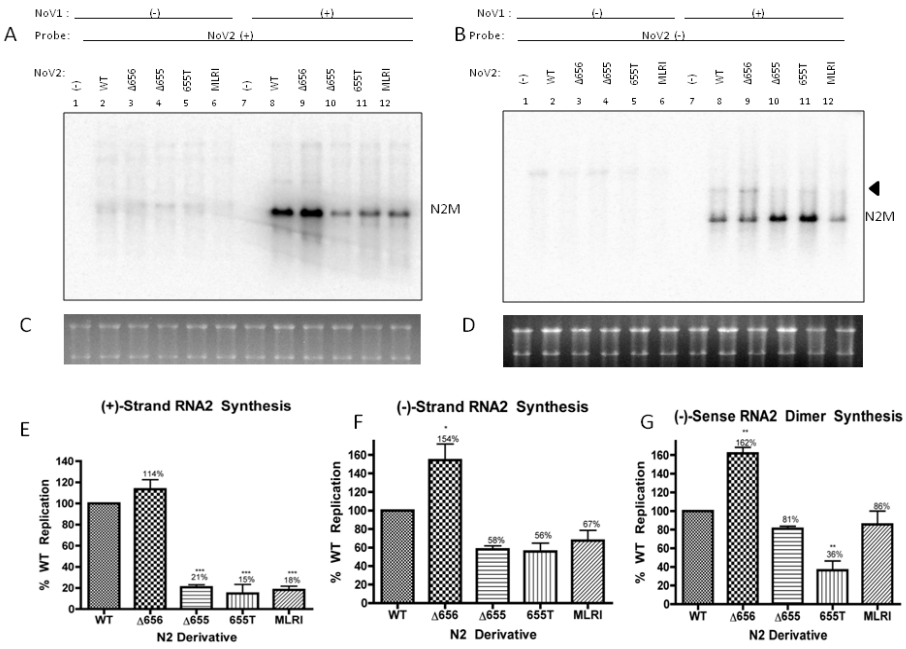

Figure 25: An upstream sequence is implicated in RNA replication. Shown are representative Northern blots probing total cellular RNA for the presence of either the positive or negative strands of RNA2 (**A** and **B**, respectively). The bold arrow represents dimeric RNA2 species, while monomeric species are indicated by N2M. **C** and **D**, images of the ethidium bromide-stained ribosomal RNAs taken immediately after electrophoresis and before transfer, used to normalize the amount of RNA loaded per lane. Quantitiave analysis of blots probing for monomeric positive strand RNA2 (**E**), monomeric negative strand RNA2 (**F**) and dimeric negative strand RNA2 (**G**) species are shown. Graphs indicate the mean of independent experiments and the standard deviation. Statistical analysis was conducted with one-way ANOVA and a Tukey's range post test (α = 0.01).

Surprisingly, deleting five of the nucleotides predicted to be involved in this interaction (NoV2-Δ656) resulted in positive strand synthesis 114% relative to WT levels (Figure 25E). We observed a significant increase in the amount of negative strand RNA2 present as well, 154% of WT (Figure 25F). The increase in negative strand templates most likely resulted in the higher-than WT values seen for genomic RNA synthesis. Synthesis of negative strand dimers was also significantly increased, as we detected 162% relative to WT (Figure 25G). It is interesting that these upstream, nucleotides that are predicted to interact with those in the loop of the 3'SL also affect synthesis of the negative strand dimers.

We wondered whether the UR in NoV2-Δ656 could have reverted back to the WT sequence, perhaps by inserting additional nucleotides into the deletion, and thereby contributing to the observed phenotype, We therefore conducted reverse transcription PCR (RT-PCR) analysis on total cellular RNA from cells transfected with plasmids pNoV1 and pNoV2-Δ656 using primers specific to RNA2. However, DNA sequence analysis of twelve clones confirmed that the original deletion was still present in all of these clonal isolates (Table 4).

Other mutations were also present, although this was not unexpected in light of the high error rate inherent in RdRp's due to their lack of proofreading activity. Of the eighteen observed mutations, eight were U to C transversions. Furthermore, half of all of the observed mutations substituted an alternative base for uridine, potentially suggesting a nucleotide bias or apparent selective pressure on viral RNA replication. It is possible to speculate that these mutations are perhaps a compensatory strategy used by the viral RNA replication machinery to offset the detrimental effects of deleting

this pentanucleotide sequence, although the effects of several mutations in a single clone make pinpointing the responsible mutation(s) difficult. We have begun to reconstruct these mutations independently into a WT background, which will permit for individual functional analysis of these changes.

Table 4: Isolated clones from cells transfected with NoV cDNAs

Clone	Mutations	Deletion Present?
NoV2Δ656-1	C1023U, ΔC742, ΔG942	Y
NoV2Δ656-2	C1010U	Y
NoV2Δ656-3	U1026C	Y
NoV2Δ656-4	A569G	Y
NoV2Δ656-5	G792C, U946C	Y
NoV2Δ656-6	U985A	Y
NoV2Δ656-7	N/A	Y
NoV2Δ656-8	N/A	Y
NoV2Δ656-9	A61U, U195C, U489C, U953G	Y
NoV2Δ656-10	U744C	Y
NoV2Δ656-11	G1284C	Y
NoV2Δ656-12	U770C, U797C, U1293C	Y

In order to verifiably implicate the UR in pseudoknot formation with the 3'SL, we considered it necessary to delete all six nucleotides predicted by our collaborators to be involved in LRI pseudoknot formation. To our surprise, deletion of these six nucleotides caused a significant decrease in positive-strand synthesis, only 21% of WT levels (Figure 25E). The deletion of one extra base caused over a five-fold decrease in RNA accumulation as compared to the Δ656 deletion. The 42% decrease in monomeric negative-strand accumulation (58% of WT) was not found to be statistically significant (Figure 25F). Therefore, while RNA replication intermediates were indeed synthesized at approximately three-fifths of WT levels, these RNA templates appeared to be incapable of being used for amplification of positive strand RNA. The synthesis of

negative strand dimers was not significantly affected, as we detected 81% of WT levels (Figure 25G). We then examined whether the putative LRI was sequence specific with the previously described NoV2-655T mutation. The average level of positive strand synthesis was only 15% relative to WT (Figure 25E). As with the NoV2-Δ655 mutation, synthesis of negative-strands was only moderately reduced, 56% of WT levels (Figure 25F). Dimer synthesis showed a significant decrease to 36% of WT levels (Figure 25G). The NoV2-655T mutation appears to be able to synthesize negative strand RNA from positive-sense RNA templates, yet it can neither (i) replicate these negative strand monomers nor (ii) synthesize negative strand dimers. Given the fact that both NoV2-Δ656 and NoV2-Δ655 were able to competently synthesize negative strand dimers, the defect in NoV2-655T dimer synthesis might suggest that the NoV2-655T mutant upstream sequence may be deleterious, perhaps interfering with RNA-RNA or RNA-protein interactions in a sequence specific manner.

By introducing the 655T mutation onto the NoV2-TL background, we generated NoV2-MLRI (*m*utant *LRI)*. We expected to see RNA replication restored to near WT levels, yet combination of these complementary sequences failed to rescue positive strand RNA synthesis. This mutant directed accumulation of 18% of WT-levels of positive strand RNA (Figure 25E), comparable to the NoV2-Δ655 and NoV2-655T mutants. Also similar to these mutations, NoV2-MLRI synthesized only a moderately reduced level of negative strand RNA, 67% of WT (Figure 25F). Synthesis of the negative strand dimer was largely unaffected, averaging 86% of WT levels (Figure 25G).

Therefore, we can conclude that this hexanucleotide sequence must play a crucial role in regulating RNA replication, although the exact nature of that role remains to be determined. We wondered whether other nodaviruses shared sequence homology to this upstream region. BLAST analysis with ClustalW sequence analysis software (Goujon, *et al.*, 2010; Larkin *et al.*, 2007) indicates phylogenetic conservation of the sequence 5'-GUU-3' from this region across the entire family *Nodaviridae* (Figure 26A). Similarly, alignments generated with Kalign (Lassmann and Sonnhammer, 2005) and MAFFT (Katoh, *et al.*, 2002) software show complete conservation of the sequence 5'-AGAUGG-3' for NoV, FHV and BBV, possibly suggesting a functional relevance associated with this region (Figure 26C). Indeed, several studies have documented the relative frequency of spontaneous deletions from nodaviral RNA2 molecules (Ball and Li, 1993; Li and Ball, 1993; Zhong *et al.*, 1992). Surprisingly, none of these reports observed the spontaneous deletion of this conserved region during serial passage of RNA2 in cells (Figure 26B), suggesting that this region may be critical for replication competency. Li and Ball (1993) reported that an FHV RNA2 molecule lacking this region could be synthetically engineered and replicated, but it is interesting that FHV naturally maintains this upstream region even under selective pressure. It is possible that this region comprises an as yet unidentified *cis* element that greatly facilitates RNA replication and possibly gene regulation of full length RNA2. Indeed, previous work with FHV identified an internal *cis*-acting RNA replication element between nucleotides 538-616 of RNA2 (Ball and Li, 1993); however, no previous work has yet examined the role of NoV RNA2 nucleotides 655-660 in RNA replication competency. It is interesting, then, that an internal region

approximately 650 nucleotides upstream of a 3' UTR *cis*-acting replication element is also required to generate WT levels of RNA2 replication in the context of full-length RNA2. Our work has successfully extended our previous findings (Rosskopf *et al.*, 2010) into full-length RNA2, and shown that sequences elsewhere in the RNA molecule are responsible, at least in part, for generating WT levels of RNA2 replication.

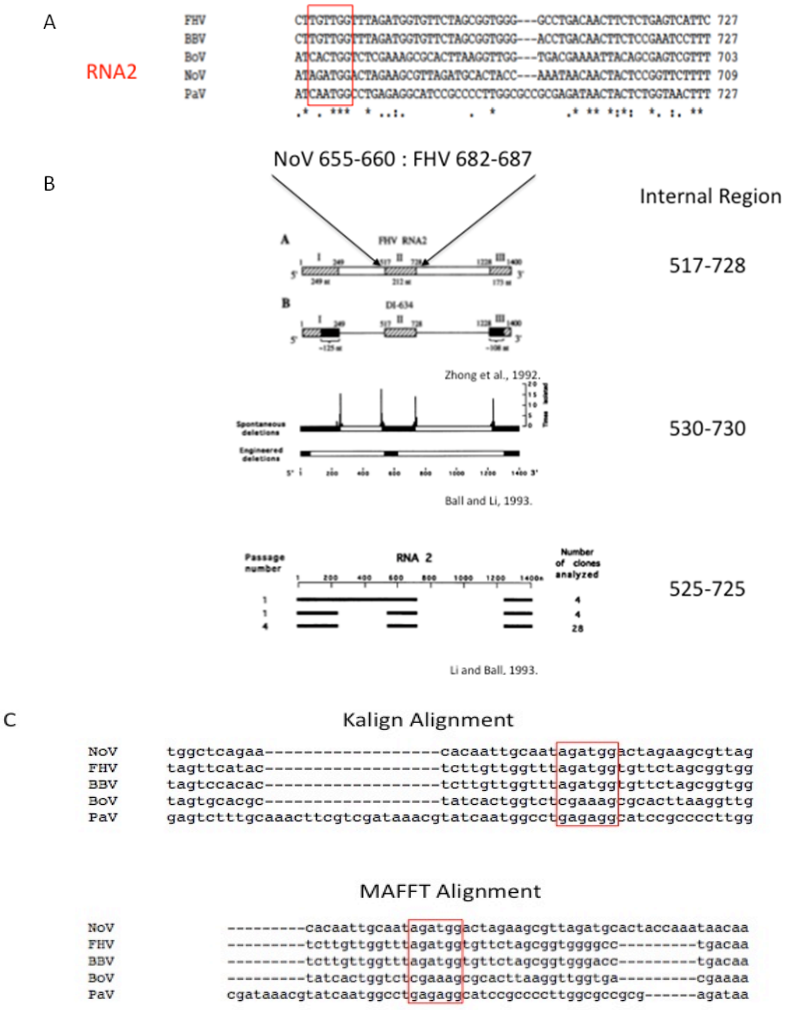

Figure 26: Phylogenetic analysis and relative stability of the predicted upstream region across the alphanodavirus genus. A, ClustalW primary sequence alignment of alphanodavirus RNA2. The red box highlights the purported upstream region of the pseudoknot. Below is shown the position of the homologous region in FHV. **B**, Diagram showing the relative constancy of the upstream region in three separate studies of FHV RNA2 undergoing serial passaging. The Internal Region was never found to be spontaneously deleted during passaging. Figures from *Zhong et al,* 1993; *Ball and Li,* 1993; *Li and Ball*, 1993. **C,** cDNA sequences from the five alphanodaviruses were analyzed with Kalign and MAFFT alignment programs. The boxed regions indicate the hexanucleotide sequence under investigation.

4.8 The 3'-terminal ten nucleotides of RNA2 appear to play a role in genome reactibility and stability.

Consistently in our predictions of NoV RNA2 3' UTR structure, we have identified a potential 3'-terminal SL at the extreme 3' end of the RNA molecule (3'10SL; Figure 27A). This structure, consisting of a three base-pair stem and a tetraloop, is hypothesized to form stably, with a predicted ΔG of -1.4 kcal/mol. We hypothesize that it might function as a steric block toward genome reactibility. Indeed, a similar structure has been previously predicted for NoV RNA2 (Kaesberg *et al.*, 1990), although its functional purpose was considered to merely play a part in the preclusion of NoV reassortment with other nodaviruses. To determine the function of these 3'-terminal ten nucleotides of NoV RNA2 on the viral replicative cycle, we deleted them from the RNA2 full-length clone, generating NoV2-Δ3'10SL, which was predicted to leave nucleotides 1323-1326 single stranded (Figure 27B).

We began our investigations by examining the importance of the 3'10SL in providing genome integrity. Conducting *in vitro* transcription using pNoV2 as a template generates full-length transcripts of RNA2 (Johnson *et al.*, 2003). These RNAs were incubated at 28^{o}C for up to 24 hours and resolved by denaturing formaldehyde-agarose gel electrophoresis. *In vitro* transcription of WT RNA2 yielded two species of RNA, which most likely represent two distinct RNA2 molecules in which the *Hepatitis delta virus* antigenomic ribozyme (HDV Rz) either successfully cleaved, generating full-length RNA2 with an authentic 3' end, or failed to cleave, resulting in a higher molecular weight chimeric RNA that contains the uncleaved ribozyme (Johnson *et al*., 2003; Price *et al*., 2005). WT RNA2 showed degradation during the 24-hour incubation (Figure 27C,

right), as evidenced by the decrease in band intensity of the lower molecular weight species, which suggests that the viral RNA is subject to spontaneous degradation during this time period. The band intensity of the chimeric RNAs showed little to no decrease; interestingly, the chimeric RNA appears to be more stable *in vitro* than WT RNA2.

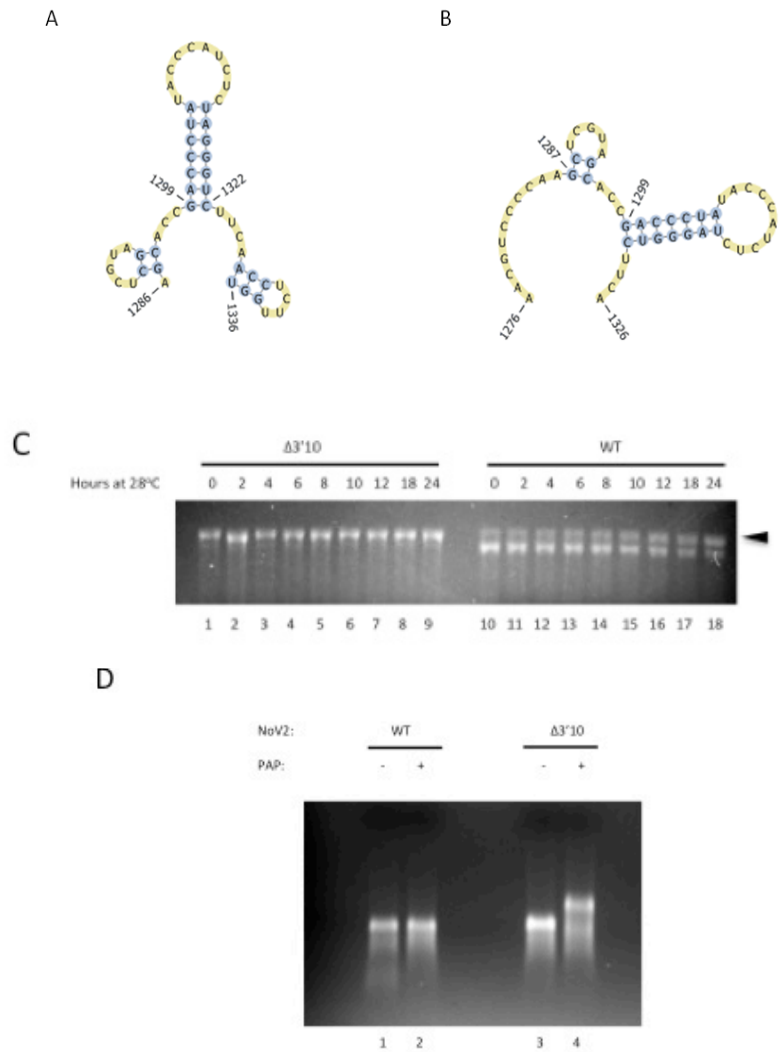

Figure 27: The 3'-terminal 10 nucleotides of RNA2 are involved in genome stability and reactivity. **A**, mfold analysis of the 3'-terminal 50 nucleotides of WT RNA2 (**A**) and NoV2-ΔSBP viewed with PseudoViewer. **B,** Deleting the 3'-terminal 10 nucleotides is predicted to leave bases 1323-1326 single-stranded. **C,** An ethidium-bromide staining of *in vitro* transcribed WT (Lanes 1-9) and mutant (Lanes 10-18) RNA2 incubated at 28°C for the indicated periods of time. The bolded arrow head denotes transcripts in which the HDV antigenomic ribozyme failed to cleave. **D**, *In vitro* transcribed RNAs were incubated in the presence or absence of poly(a) polymerase and analyzed by denaturing agarose gel electrophoresis. Lanes 1 and 3 represent mock reactions in which template RNAs were incubated in reaction buffer supplemented with ATP.

Surprisingly, the NoV2-Δ3'10SL RNAs showed only a singular RNA species, which could represent chimeric RNA molecules in which the HDV Rz did not cleave (Figure 27C, left). While it is remotely possible that deletion of the 3'10SL affects the

ability of the HDV Rz to self-cleave, it is plausible to hypothesize that the transcripts in which the HDV Rz successfully cleaved were immediately and completely degraded upon synthesis. This would suggest that the mutant RNA is extremely unstable and subject to spontaneous degradation. The data so far do not conclusively support either hypothesis, and therefore, current investigations are underway to quantify the rate of decay of WT RNA and the relative stability of the chimeric mutant. If this structure is involved in genome integrity, it may intrinsically function to shield the genome from insult such as degradation by ribonucleases, perhaps by precluding its interaction with cellular proteins.

We next considered the possible role of this structure in protecting the genome from enzymatic modification, for example by poly(A) polymerase or RNA ligase. We assayed the reactibility of WT and Δ3'10SL versions of NoV RNA2 to *in vitro* polyadenylation with *E. coli* poly(A) polymerase (PAP), previously shown to be unsuccessful for other nodavirus RNAs (Dasgupta and Sgro, 1984; Dasmahapatra *et al.*, 1985; Guarino *et al.*, 1984). Gel electrophoresis of these RNAs indicated that WT NoV RNA2 is indeed blocked to modification by PAP (Figure 27D, left). The presence of lower molecular weight species of RNA2 treated with PAP might be due to polyadenylation of prematurely terminated transcripts by the T7 RNA polymerase during *in vitro* transcription. Indeed, if full-length WT RNA2 were modified by PAP, one would expect to see species of molecular weights higher than the full-length RNA2, yet none were detected.

We did, however, observe higher molecular weight species of RNA when NoV2-Δ3'10 was reacted with PAP (Figure 27D, right). This new species of RNA could

potentially be a polyadenylated version NoV RNA2 molecule. Careful analysis of these results indicates that some mutant RNAs remain unreacted, as there is a small area of density near the expected molecular mass of unreacted control RNA. The higher molecular weight species may represent an 'upper limit' to polyadenylation, as any further adenylation of the genome could cause instability and subsequent degradation. Alternatively, perhaps those RNAs that received the most adenylate residues are fewer in number, and therefore, more difficult to detect with these techniques. Importantly, the negative controls in this experiment represent mock reactions in which the RNA substrates were incubated in reaction buffer in the presence of ATP; any differences observed between control and experimental samples must be attributed solely to the presence of PAP. Further testing is underway to verify the nature of these higher molecular weight RNAs.

Chapter 5

DISCUSSION

5.1 Functional analysis of the RNA2 3'SL in transfected mammalian cells

Herein, we have shown that the NoV RNA2 3'SL element retains both structural and sequence requirements for directing RNA replication. Our data suggest that the 3'SL acts as a *cis*-acting RNA replication element in full-length RNA2 in the context of mammalian cells. This work is in agreement with our previous report (Rosskopf *et al.*, 2010) in which we implicated the 3'SL as a *cis*-acting RNA replication element in RNA replicons in transformed yeast. Further, using full-length RNA2 has allowed us to implicate another *cis*-region involved in the regulation of RNA2 replication. The fact that the SL also functions in full-length RNA2 could imply that the structure is critical for RNA replication during a natural infection as well.

It is plausible that during the course of negative strand synthesis from a positive-strand template, the RdRp may fail to terminate transcription at the appropriate point, bind to another RNA2 molecule *in trans* or the same template *in cis*, and without releasing the nascent strand, continue synthesis on the new template, producing a negative strand dimer. Both FHV and NoV were found to synthesize head-to-tail homodimers and heterodimers of RNA2 (Albariño *et al.*, 2001; Johnson *et al.*, 2003; Price *et al.*, 2005), as mentioned previously in the Background. Indeed, the FHV RdRp has been shown to be able to switch templates during RNA transcription, which would facilitate dimer formation (Ball and Li, 1993).

The present work has shown that the stem of the 3'SL must remain double-stranded to support RNA replication. Interestingly, mutations in which basepairing

interactions are disrupted, such as NoV2-Up, NoV2-Down, NoV2-S1T, show an interesting trend of serving as poor substrates for monomeric positive strand RNA synthesis. Accordingly, mutations in which the stem was allowed to basepair, as with mutations NoV2-Dbl and NoV2-DST, rescued RNA replication to near-WT levels. Perhaps, then, the RdRp requires a large structural moiety near the 3'-terminus of the RNA molecule, and will naturally select templates that contain either the WT 3'SL structure or a mutated variant such NoV2-S2T. Indeed, this would account for the observed phenotypes of the NoV-S2T mutation (Figure 14). While the structural substitution did not abrogate RNA replication, it is interesting to note that similar nucleotides were involved in forming double-stranded stems in both WT and S2 transversion sequences (nucleotides 1316-1322). Additionally, of the ten nucleotides in the WT loop, only three nucleotides, 1310, 1311 and 1315, were predicted to convert from single-stranded in WT RNA2 to double-stranded in NoV2-S2T. As such, it is possible that if the sequence of the loop were to necessarily remain single-stranded in order to direct RNA replication through RNA-protein or RNA-RNA interactions, this interaction could perhaps still occur in the NoV2-S2T mutation. This structure perhaps has a large three-dimensional footprint that allows the RdRp to select this RNA as a template, allowing RNA replication to continue with only minimal disruption.

In support of this hypothesis, the NoV2-ΔSBP mutant failed to synthesize both monomeric strands of RNA2, presumably because the stability of this mutant stem sequence is insufficient to properly exhibit the nearest neighbor nucleotides in the loop for further interaction. It is possible that the mutation of four base pairs from G-C to A-U, four strong-to-weak substitutions, allowed greater flexibility in the stem, leading to the

modest reduction of RNA accumulation. This ‘breathing’ is an important occurrence in RNA-RNA interactions, and can even aid in structural resonance (Wyatt *et al.*, 1990). These observations might suggest that the 3’SL is at least one-component of a multivariable process responsible for the creation of dimeric RNA2. Likewise, the mutations that allowed 3’SL formation only in a single polarity of RNA2 (NoV2-S1neg and NoV2-S2pos) were similarly incapable of positioning nearby nucleotides for further interaction, suggesting that stability of the entire structure is required in order to properly signal and coordinate RNA replication.

According to this hypothesis, the nucleotides in the stem of the 3’SL would necessarily remain double-stranded in order to appropriately position the single-stranded loop nucleotides. As shown in Figure 22, both loop size and sequence are important factors for RNA2 replication. When the loop decreases in size, synthesis of monomeric and dimeric RNA forms of RNA2 decreases as well, with the 3Loop mutant perhaps representing a minimal level of RNA replication. Interestingly, the ΔLoop mutation led to near WT-levels of RNA2 replication. Accounting for the likely three-dimensional structure of the mutant, which is predicted to be a tetraloop, the sequence of the loop, in this case 5’-UAUA-3’, could harbor elements beneficial to RNA replication. Alternatively, if transient thermodynamic breathing in the 3’SL stem allowed for further modification to the loop, it is possible that the base pair between C1303 and G1318 also is interrupted, leading to a hexaloop with the sequence 5’-CUAUAG-3’. According to our model, we predict that this mutation would most likely replicate better than NoV2-4Loop, yet not as efficiently as NoV2-TL. Because NoV2-ΔLoop replicates to

higher levels than even NoV2-TL, we argue that the sequence of this mutant must be responsible for directing RNA replication to the observed levels.

The nucleotides that comprise the 3'SL loop are conserved in sequence with a similarly predicted stem loop structure in the 3' UTR of NoV RNA1 (Melendez, Rosskopf and Johnson, unpublished results). This conservation led us to believe that the nucleotides in the loop must be involved in either RNA-RNA or RNA-protein interactions that are critical for RNA replication. It would be plausible for this *cis*-acting RNA replication element, or some other interacting region, to act as the viral or host factor-binding site in the genomic sense RNA, as this would allow for the 5' to 3' synthesis of the negative strand RNA replication intermediate, as has been shown for other positive-strand RNA viruses (Miller *et al*, 1986; Cui & Porter, 1995). Alternatively, this sequence may occur in a negative strand RNA molecule, possibly in a homodimer, and allow for the synthesis of a positive strand RNA.

Following this argument, we considered it likely that the loop may be involved in RNA-RNA interactions. Indeed, the hexanucleotide sequence predicted to be involved in formation of a long-range interaction (LRI) with the 3'SL loop (Figure 23) was also implicated in RNA2 replication. The deletion of all six nucleotides predicted to be involved in this putative LRI (NoV2-Δ655) led to a significant decrease in synthesis of both positive and negative strand forms of RNA2. Even base substitutions (NoV2-655T) in which the 3'SL was left WT exhibited significant decreases in RNA accumulation. Further, covariation mutagenesis (NoV2-MLRI) was unable to rescue replication to near WT levels. This suggests that the upstream 655T mutation is more deleterious than even a transverse loop sequence (Figure 22). Surprisingly, deleting five of the six

nucleotides predicted to be involved in the LRI (Δ656) did not abrogate RNA replication as predicted by our hypothesis. A possible explanation of these results could be that A655 may be involved in RNA-protein or other RNA-RNA interactions. If this residue were to be required for the intermolecular interaction to occur, it is plausible that its deletion could inhibit RNA replication. Incidentally, it is interesting to consider whether the nucleotides immediate upstream of this nucleotide are also involved in RNA replication. Alternatively, the nucleotides downstream of A655 may not participate in this putative structural interaction, and the sole responsible element of the upstream region may be A655, and possibly other upstream nucleotides.

Therefore, our working hypothesis posits that the 3'SL functions as a core promoter while the ancillary upstream region acts as an enhancer element. The role of this sequence then becomes to base pair with the 3'SL and aid in positioning the RdRp over the initiation site. Indeed, work with bacteriophage Qβ has demonstrated that a sequence approximately 1200 nucleotides upstream of a SL structure that lies near the 3' end of Qβ genomic RNA participates in a long-range interaction with this SL to promote RNA replication (Klovins *et al.*, 1998, Klovins and van Duin, 1999). For Qβ, this upstream site serves as an RdRp-binding site that aids in positioning the RdRp over this structure for initiation of RNA replication. We consider it is possible that the NoV2-TL mutation disrupts either RNA-RNA or RNA-protein interactions in a sequence-specific manner, thus leading to the observed defect in replication competency of the template RNA. Specifically, the promoter function of the NoV RNA2 3'SL may be altered such that binding to ancillary replication factors, presumably co-opted host RNA-binding proteins (RBPs), or perhaps the viral RdRp.

Further, we hypothesize that this region is homologous to the internal region studied in FHV (Ball and Li, 1993; Li and Ball, 1993) responsible for aiding RNA replication through serial replicative passages in transfected cells, and that the primary sequence and secondary structure of this region are both critical for coordinating RNA replication. If this region were to serve as an RdRp-binding site, deletion of all nucleotides involved in RdRp binding, such as A655 and the preceding nucleotide, would lead to a loss of RNA2 replication. Furthermore, it is possible that by mutating the binding-site sequence, an RNA-protein interaction is disrupted, as in the NoV2-655T mutant, even in the presence of a covaried SL (NoV2-MLRI). It would be interesting to test whether alternative substitutions for A655 would similarly inhibit RNA replication.

We therefore propose the following four-step mechanism for synthesis of positive strand monomers from a dimeric negative strand template (Figure 28). The first step may follow one of two routes: (step 1a) RNA tertiary domain folding causes the upstream copy of the 3'SL to basepair with the downstream copy of the region predicted to be involved in an LRI (RNA-RNA interaction) or (step 1b) the RdRp or a host-derived cofactor binds to the downstream copy of the 3'SL in a sequence specific manner (RNA-protein interaction). Essentially, the only difference between these two alternatives is whether the RNA first folds to form a pseudoknot or whether the RdRp binds to its cognate binding site before translocation to the relevant copy of the 3'SL. In either case, the second step is to translocate the RdRp into close proximity with 3'SL at the 3' end of the upstream copy of RNA2. Presumably, the RdRp is now sufficiently close to the dimer junction, a mere fourteen nucleotides downstream from 3'SL, that the third step can be initiated. In this third step, the RdRp would translocate to the initiation

site near the 3'-terminus of the upstream copy of RNA2 (just upstream of the dimer junction). The fourth and final step would be synthesis of monomeric, positive strand RNA from the dimeric negative strand template.

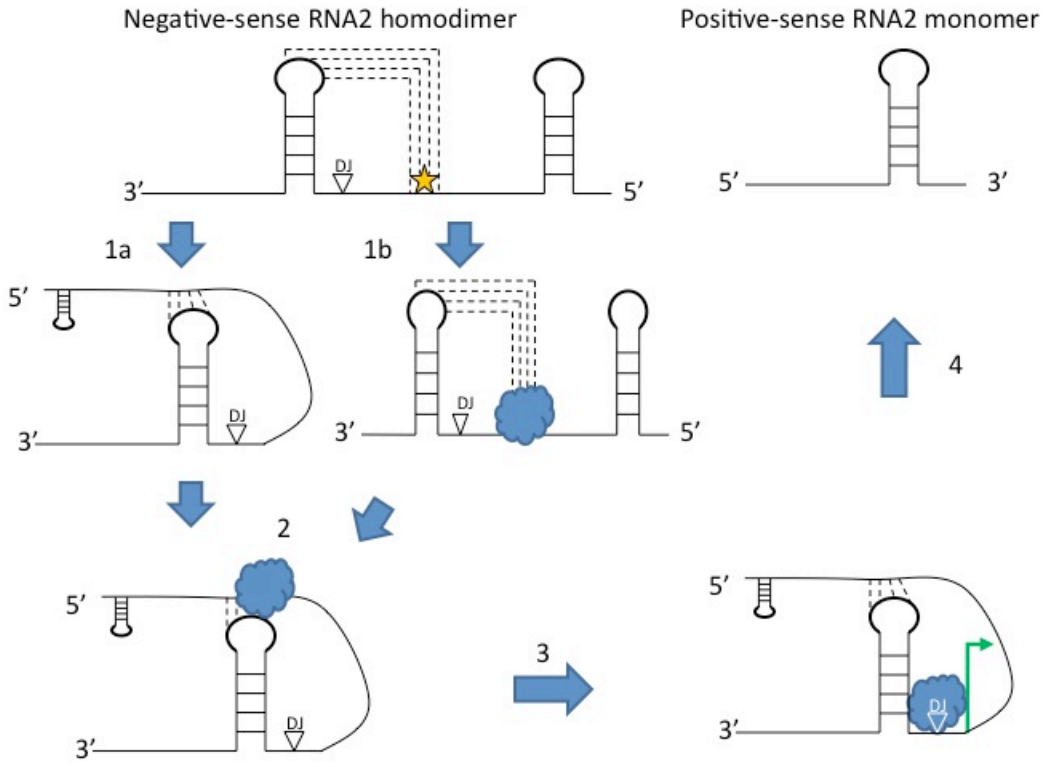

Figure 28: A proposed mechanism for the synthesis of positive strand RNA2 from dimeric, negative-strand RNA2 templates. Shown at top is a negative strand RNA2 homodimer that allows for the putative interaction (dashed lines) between the 3'SL and the upstream region (gold star). The dimer junction (DJ, open arrow head) is only fourteen nucleotides downstream of 3'SL. The first step allows RNA folding to create a pseudoknot between these two substituent regions (1a) or for RdRp binding at the RdRp binding site (1b). In either case, the RNA must fold such that the RdRp is brought in close proximity to 3'SL, allowing it to translocates to the dimer junction (3) and initiate RNA resolution (green arrow). At the end of the replicative cycle, monomeric, positive-strands RNA2 replication products are ready for subsequent translation or packaging (4).

We propose to test this hypothesis by engineering synthetic RNA2 dimer molecules in which the upstream or internal copy of the 3'SL is deleted while the downstream copy remains. We would expect this synthetic RNA to be unable to

synthesize monomeric positive strand RNA2, in accordance with our hypothesis. The presence of RNA2 positive strand monomers derived from this template could suggest two outcomes. First, other sequences near the junction may fold to create a structural alternative for the WT SL, allowing resolution of RNA2 monomers. Alternatively, it is possible that an alternative model of dimer resolution, and even the role of dimers in the NoV life cycle, better explains the synthesis of monomeric positive strand RNA2.

Our work has also demonstrated a functional relevance associated with another predicted SL structure at the extreme 3'-terminus of RNA2 (3'10SL; Figure 27). It is interesting that this structure is potentially involved in protecting the genome from modification. The importance of this predicted structure could be an intrinsic characteristic of the natural NoV replication cycle. Recent investigations in our laboratory have localized NoV replication complexes to the outer mitochondrial membrane (Gant *et al.*, manuscript in preparation). The natural eukaryotic host of NoV segregates many, but not all, RNA processing activities to the nucleus; because nodaviruses replicate in the cytoplasm, it is likely that nodaviral RNAs only rarely encounter cytoplasmic polyadenylation machinery during natural infection. Therefore, we hypothesize that the primary function of this structure involves genome stability *in vivo* or translation of the RNA and that blockage of the terminus from enzymatic modification may be less important *in vivo*.

Alternatively, it is possible that this structure may participate in RNA-protein interactions in a sequence specific manner; essentially, this putative stem loop would be responsible for recruiting host or viral RBPs.

CHAPTER 6

CONCLUSIONS

In this work, we have demonstrated specific structural requirements of the *Nodamura virus* RNA2 3'-untranslated region stem loop for directing RNA replication of full-length RNA2 *in vivo*. We have thus so far demonstrated that sequence specificity of the stem is not a requirement for stem loop formation, and that base pairing interactions are required for RNA replication to occur. The single-stranded loop region retains strict structural and sequence requirements to conduct WT levels of RNA replication. Additionally, the 3'SL functions as a *cis*-acting RNA replication element in both polarities of the RNA. The regions associated with the predicted long-range interaction are also implicated in RNA synthesis, although the mechanism through which is not yet understood, although we hypothesize that they may be implicated in RNA-RNA interactions. Finally, the 3'-terminal ten nucleotides of RNA2 are involved in genome stability, resistance to modification and RNA replication. Our work herein has important implications for a variety of experiments. Characterizing the 3'SL may aid in establishment of an *in vitro* NoV-based replication system by defining the minimal elements required for RNA replication. Further, this system could allow for discovery of cellular RNA-binding proteins that interact with the 3'SL. Finally, defining the structural and functional characteristics of the 3'SL may aid in discovery of the method of NoV RNA replication initiation. RNA structure is critically important for a wide variety of viral functions, and our work sheds light onto several intriguing aspects of the *Nodamura virus* life cycle.

REFERENCES

1. Albariño, C.G., Price, B.D., Eckerle, L.D., Ball, L.A., 2001. Characterization and template properties of RNA dimers generated during Flock house virus RNA replication. Virol. 289 (2): 269-282.

2. Albariño, C.G., Eckerle, L.D., Ball, L.A., 2003. The cis-acting replication signal at the 3' end of Flock house virus RNA2 is RNA3-dependent. Virol. 311 (1): 181-191.

3. Antao, V.P., Lai, S.Y., Tinoco Jr., I. 1991. A thermodynamic study of unusually stable RNA and DNA hairpins. Nucl. Acids Res. 19 (21): 5901-5905.

4. Bailey, L., Newman, J.F., Porterfield, J.S., 1975. The multiplication of Nodamura virus in insect and mammalian cell cultures. J Gen Virol, 26 (1): 15-20.

5. Ball, L.A. 1995., Requirements for the self-directed replication of Flock House virus RNA 1. J. Virol. 69 (2): 720-727.

6. Ball, L.A., Amann, J.M., Garrett, B.K., 1992. Replication of Nodamura virus after transfection of viral RNA into mammalian cells in culture. J Virol. 66(4):2326-34.

7. Ball, L.A., Li, Y., 1993. cis-acting requirements for the replication of flock house virus RNA 2. J. Virol. 67 (6): 3544-3551.

8. Ball, L.A., Johnson, K.L. 1998. Nodaviruses of insects. In: Miller, L.K., Ball, L.A. (Eds.), The Insect Viruses. Plenum Publishing Corporation, New York, pp. 225-267.

9. Brierley, I., Pennel, S., Gilber, R.J.C. 2007. Viral RNA pseudoknots: versatile motifs in gene expression and replication. Nature 5: 598-610.

10. Brion, P., Westhof, E., 1997. Hierarchy and dynamics of RNA folding. Ann. Rev. Biophys. & Biomolec. Struc. 26 (1): 113-137.

11. Buchholz, U.J., Finke, S., Conzelmann, K. 1997. Generation of Bovine respiratory syncytial virus (BRSV) from cDNA: BRSV NS2 is not essential for virus replication in tissue culture , and the human RSV leader region acts as a functional BRSV genome promoter. J. Virol 73 (1): 251-259.

12. Cai, D., Qiu, Y., Qi, N., Yan, R., Lin, M., Nie, D., Zhang, J., Hu, Y., 2010. Characterization of Wuhan Nodavirus subgenomic RNA3 and the RNAi inhibition property of its encoded protein B2. Virus Res. 151 (2): 153-160.

13. Chao, J.A., Lee, J.H., Chapados, B.R., Debler, E.W., Schneeman, A., Williamson, J.R., 2005. Dual modes of RNA-silencing suppression by *Flock house virus* protein B2. J. Struc. & Mol. Biol. 12: 952-957.

14. Cui, T., Porter, A.G., 1995. Localization of binding site for Encephalomyocardidits virus RNA polymerase in the 3'-noncoding region of the viral RNA. Nucl. Acids. Res. 23 (3): 377-382.

15. Dasgupta, R., Sgro, J.Y., 1984. Nucleotide sequences of three Nodavirus RNA2's: the messengers for their coat protein precursors. Nuc. Acids Res. 17 (18): 7525-7526.

16. Dasmahapatra, B., Dasgupta, R., Ghosh, A., Kaesberg, P., 1984. Structure of the black beetle virus genome and its functional implications. J. Mol. Biol. 182 (2): 183-189.

17. Decroly, E., Ferron, F., Lescar, J., Canard, B., 2012. Conventional and unconventional mechanisms for capping viral mRNAs. Nat. Rev. Micro. 10: 51-65.

18. Deiman, B.A.L.M., Pleij, C.W.A. 1997. Pseudoknots: a vital feature in viral RNA. Sem. In Virol. 8: 166-175.

19. Dirks, R.M., Pierce, N.A., 2003. A partition function algorithm for nucleic acid secondary structure including pseudoknots. J. Comput. Chem. 24 (13): 1664-1677.

20. Dirks, R.M., Pierce, N.A., 2004. An algorithm for computing nucleic acid base-pairing probabilities including pseudoknots. J. Comput. Chem 25 (10): 1295-1304.

21. Draper, D.E., 1996. Strategies for RNA folding. Trends in Biochem. Sci. 21 (4): 145-149.

22. Draper, D.E., 2008. RNA folding: thermodynamic and molecular descriptions of the roles of ions. Biophys J. 95 (12):

23. Dreher, T.W., 2009. Role of tRNA-like structures in controlling plant virus replication. Virus Res. 139 (2): 217-229.

24. Eckerle, L.D., Ball, L.A. 2002. Replication of the RNA segments of a bipartite viral genome is coordinated by a transactivating subgenomic RNA. Virol. 296 (1): 165-176.

25. Eckerle, L.D., Albarino, C.G., Ball, L.A., 2003. Flock house virus subgenomic RNA3 is replicated and its replication correlates with transactivation of RNA2. Virol. 317 (1): 95-108.

26. Friesen, P.D., Rueckert, R.R., 1981. Synthesis of Black beetle virus proteins in cultured Drosophila cells: differential expression of RNAs 1 and 2. J. Virol 37 (3): 876-886.

27. Friesen, P.D., Rueckert, R.R., 1982. Black beetle virus: messenger for protein B is a subgenomic viral RNA. J. Virol. 42 (3): 986-995.

28. Gallagher, T.M., 1987. Synthesis and assembly of nodaviruses. University of Wisconsin - Madison.

29. Gardner, P.P., Giegerich, R., 2004. A comprehensive comprison of comparative RNA structure prediction approaches. BMC Bioinformatics 5: 140.

30. Garzon, S., Charpentier, G. Kurstak, E. 1978. Morphogenesis of the Nodamura virus in the larvae of the lepidopteran Galleria mellonella (L.). Archives of Virology (6): 61-76.

31. Garzon, S., Strykowski, H., Charpentier, G. 1990. Implication of mitochondria in the replication of Nodamura virus in larvae of the Lepidoptera,Galleria mellonella (L.) and in suckling mice. Archives of Virology (113): 165-176.

32. Giegé, R., Florentz, C., Dreher, T.W. 1993. The TYMV tRNA-like structure. Biochimie 75: 569-582.

33. Goujon M., McWilliam H., Li W., Valentin F., Squizzato S., Paern J., Lopez R., 2010. A new bioinformatics analysis tools framework at EMBL-EBI. Nucl. Acids Res. 38 Suppl: W695-9.

34. Guarino, L.A., Ghosh, A., Dasmahapatra, B., Dasgupta, R., Kaesberg, P. 1984. Sequence of the black beetle virus subgenomic RNA and its location in the viral genome. Virol. 139 (1): 199-203.

35. Hanley K.A., Lee J.J., Blaney J.E. Jr., Murphy B.R., Whitehead S.S. Paired charge-to-alanine mutagenesis of dengue virus type 4 NS5 generates mutants with temperature-sensitive, host range, and mouse attenuation phenotypes. J. Virol 2002;76(2):525–531

36. Holland, J. A., M. R. Hansen, Z. Du, and D. W. Hoffman. 1999. An examination of coaxial stacking of helical stems in a pseudoknot motif: the gene 32 messenger RNA pseudoknot of bacteriophage T2. RNA 5: 257-271.

37. Inoue, T., Cech, T.R., 1985. Secondary structure of the circular form of the *Tetrhymena* rRNA intervening sequence: a technique for RNA structure analysis using chemical probes and reverse transcriptase. Proc. Natl. Acad. Sci. USA 82: 648-652.

38. Iwamoto, T., Mise, K., Takeda, A., Okinaka, Y., Mori, K.I., Arimoto, M., Okuno, T., Nakai, T., 2005. Characterization of striped jack nervous necrosis virus subgenomic RNA3 and biological activities of its encoded protein B2. J. Gen. Virol. 86 (10): 2807-2816.

39. Jeng, K.-S., Daniel, A., Lai, M.M.C. 1996. A pseudoknot ribozyme structure is active in vivo and required for hepatitis delta virus RNA replication. J. Virol. 70 (4): 2403-2410.

40. Johnson, K.L., Price, B.D., Ball, L.A., 2003. Recovery of infectivity from cDNA clones of Nodamura virus and identification of small nonstructural proteins. Virol. 305 (2): 436-451.

41. Johnson, K.L., Price, B.D., Eckerle, L.D., Ball, L.A., 2004. Nodamura virus nonstructural protein B2 can enhance viral RNA accumulation in both mammalian and insect cells. J. Virol. 78 (12): 6698-6704.

42. Johnson, K.N., Zeddam, JL., Ball, L.A., 2000. Characterization and construction of functional cDNA clones of *Pariacoto virus*, the first Alphanodavirus isolated outside Australasia. J. Virol. 74 (11): 5123-5132.

43. Johnson, K.N., Johnson, K.L., Dasgupta, R., Gratsch, T., Ball, L.A., 2001. Comparisons among the larger genome segements of six nodaviruses and their encoded RNA replicases. J Gen. Virol. 82 1855-1866.

44. Joshi, S. Joshi, R.L., Haenni, A.-L., Chapeville, F. 1983. tRNA-like structures in genomic RNAs of plant viruses. Trend. In Biochem. Sci. 8 (11): 402-404.

45. Kaesberg, P., Dasgupta, R., Sgro, J. Y., Wery, J. P., Selling, B.H., Hosur, M.V., Johnson, J.E., 1990. Structural homology among four nodaviruses as deduced by sequencing and X-ray crystallography. J. Mol. Biol. 214 (2): 423-435.

46. Katoh, K., Misawa, K., Kuma, K.I., Miyata, T., 2002. MAFFT: a novel method for rapid multiple sequence alignment based on fast Fourier transformation. Nucl. Acids Res. 30 (14): 3059-3066.

47. King, A.M.Q., Adams, M.J., Carstens, E.B., Lefkowitz, E., 2011. Virus Taxonomy: Ninth Report of the International Committee on Taxonomy of Viruses, first ed. Waltham, MA.

48. Klovins, J., Berzins, V., van Duin, J., 1998. A long-range interaction in Qbeta RNA that bridges the thousand nucleotides between the M-site and the 3' end is required for replication. RNA 4: 948-957.

49. Klovins, J., van Duin, J. 1999. A long-range pseudoknot in Qβ RNA is essential for replication. J. Mol. Biol. 294 (4): 875-884.

50. Kolk, M.H., van der Graaf, M., Wijmenga, S.S., Pleij, C.W.A., Heus, H.A., Hilbers, C.W., 1998. NMR structure of a classical pseudoknot: interplay of single-and double-stranded RNA. Science 280 (5362): 434-438.

51. Kopek, B. G., Settles, E. W., Friesen, P.D., Ahlquist, P. 2010. Nodavirus-induced membrane rearrangement in replication complex assembly requires replicase protein A, RNA templates and polymerase activity. J. Virol 84 (24): 12492-12503.

52. Kürber, S., Ali, S.S., Julian, C.H., 2009. Structure of the RNA-binding domain of Nodamura virus protein B2, a suppressor of RNA interference. Biochemistry 48 (11): 2307-2309.

53. Lambert, D., Leipply, D., Shiman, R., Draper, D.E., 2009. The influence of monovalent cation size on the stability of RNA tertiary structures. J. Mol. Biol. 390 (4): 791-804.

54. Larkin M.A., Blackshields G., Brown N.P., Chenna R., McGettigan P.A., McWilliam H., Valentin F., Wallace I.M., Wilm A., Lopez R., Thompson J.D., Gibson T.J. and Higgins D.G., 2007. ClustalW and ClustalX version 2. Bioinformatics 23 (21): 2947-2948.

55. Lassmann, T., Sonnhammer, E.L.L., 2005. Kalign – an accurate and fast multiple sequence alignment program. BMC Bioinformatics 6: 298.

56. Lehrach, H., Diamond, D., Wozney, J.M., Boedtker, H. 1977. RNA molecular weight determinations by gel electrophoresis under denaturing conditions, a critical reexamination. Biochem. 16 (21): 4743-4751.

57. Li, H., Li, W.X., Ding, S.W., 2002. Induction and suppression of RNA silencing by an animal virus. Science 296 (5571): 1319-1321.

58. Li, W.X., Li, H., Lu, R., Li, F., Dus, M., Atkinson, P., Brydon, E.W.A., Johnson, K.L., García-Sastre, A., Ball, L.A., Palese, P., Ding, S.W., 2004. Interferon antagonist proteins of influenza and vaccinia viruses are suppressors of RNA silencing. PNAS 101 (5): 1350-1355.

59. Li, Y., Ball, L.A., 1993. Nonhomologous RNA recombination during negative-strand synthesis of flock house virus RNA. J. Virol. 67 (7): 3854-3860.

60. Lindenbach, B.D., Sgro, J. Y., Ahlquist, P. 2002. Long-distance base pairing in Flock house virus RNA1 regulates subgenomic RNA3 synthesis and RNA2 replication. J. Virol. 76 (8): 3905-3919.

61. Liu, C., J. Zhang, F. Yi, J. Wang, X. Wang, H. Jiang, J. Xu, and Y. Hu., 2006. Isolation and RNA1 nucleotide sequence determination of a new insect nodavirus from Pieris rapae larvae in Wuhan city, China. Virus Res 120:28-35.

62. Liu, Y., Wimmer, E., Paul, A.V., 2009. *Cis*-acting RNA elements in human and animal plus-strand RNA viruses. Biochimica et Biophysica Acta 1789: 495-517.

63. Longworth, J.F., Carey, G.P., 1976. A small RNA virus with a divided genome from *Heteronychus arator* (F.) [Coleoptera: Scarabaeidae] J Gen Virol 33 (1): 31-40.

64. Mans, R.M.W., Pleij, C.W.A., Bosch, L. 1991. tRNA-like structures: structure, function and evolutionary significance. Eur. J. Biochem. 201: 303-324.

65. Melchers, W.J.G., Hoenderop, J.G.J., Slot, H.J.B., Pleij, C.W.A., Pilipenko, E.V., Agol, V.I., Galama, J.M.D., 1997. Kissing of the two predominant hairpin loops in the coxsackie B virus 3' untranslated region is the essential structural feature of the origin of replication required for negative-strand RNA synthesis. J. Virol. 71 (1): 686-696.

66. Miller, W.A., Bujarski, J.J., Dreher, T.W., Hall, T.C., 1986. Minus-strand initiation by Brome mosaic virus replicase within the 3' tRNA-like structure of native and modified RNA templates. J. Mol. Biol. 187: 537-546.

67. Miller, W.A., Koev, G. 2000. Synthesis of subgenomic RNAs by positive-strand RNA viruses. Virol. 273: 1-8.

68. Morch, M.D., Joshi, R.L., Denial, T.M., Haenni, A.L., 1987. A new 'sense' RNA approach to block viral RNA replication in vitro. Nucl. Acids Res. 15 (10): 4123-4130.

69. Murphy, F.A., Scherer, W.F., Harrison, A.K., Dunne, H.W., Gary, G.W., 1970. Characterization of Nodamura virus, an arthropod transmissible picornavirus. Virol. 40, 1008-1021.

70. Newman, J.F.E., Brown, F., 1976. Absence of poly(A) from the infective RNA of Nodamura virus. J. Gen. Virol. 30 (1): 137-140.

71. Newman, J.F.E., Matthews, T., Omilianowski, D.R., Salerno, T., Kaesberg, P., Rueckert, R., 1978. In vitro translation of the two RNAs of Nodamura virus, a novel mammalian virus with a divided genome. J Virol 25 (1): 78-85.

72. Olsthoorn, R.C.L., Mertens, S., Brederode, F.T., Bol, J.F., 1999. A conformational switch at the 3' end of a plant virus RNA regulates viral replication. EMBO J. 18: 4856-4864.

73. Pinck, M., Yot, P., Chapeville, F., Duranton, H.M., 1970. Enzymatic binding of valine to the 3' end of TYMV-RNA. Nature: 226: 954-956.

74. Pleij, C.W.A., Rietveld, K., Bosch, L., 1985. A new principle of RNA folding based on pseudoknotting. Nucl. Acids Res. 13 (5): 1717-1731.

75. Pleij, C.W.A., 1990. Pseudoknots: a new motif in the RNA game. Trends in Biochem. Sci. 15 (4): 143-147.

76. Price, B.D., Eckerle, L.D., Ball, L.A., Johnson, K.L., 2005. *Nodamura virus* RNA replication in *Saccharomyces cerevisiae*: heterologous gene expression allows replication-dependent colony formation. J. Virol. 79 (1), 495-502.

77. Podder, S.K., 1971. Cooperative non-enzymatic base recognition and stability of the G—U wobble pair. Nature 232: 115-116.

78. Puglisi, J.D., Wyatt, J.R., Tinoco Jr., I., 1990. Conformation of an RNA pseudoknot. J. Mol. Biol. 214: 437-453.

79. Qiu, Y., D. Cai, N. Qi, Z. Wang, X. Zhou, J. Zhang, and Y. Hu., 2011. Internal initiation is responsible for the synthesis of Wuhan Nodavirus subgenomic RNA. J Virol 85:4440-4451.

80. Reeder, J. Giegerich, R., 2004. Design, implementation and evaluation of a practical pseudoknot folding algorithm based on thermodynamics. BCM Bioinformtics 5 (104).

81. Rietveld, K., Van Poelgeest, R., Pleij, C.W.A., Van Boom, J.H., Bosch, L., 1982. The tRNA-like structure at the 3' terminus of turnip yellow mosaic virus RNA. Differences and similarities with canonical tRNA. Nucl. Acids Res. 10 (6): 1929-1946.

82. Rietveld, K., Pleij, C.W.A., Bosch, L., 1983. Three-dimensional models of the tRNA-like 3' termini of some plant viral RNAs. EMBO 2 (7): 1079-1085.

83. Rivas, E. Eddy, S.R., 1999. A dynamic programming algorithm for RNA structure prediction including pseudoknots. J. Mol. Biol. 285: 2053-2068.

84. Rohll, J.B., Moon, D.H., Evans, D.J., Almond, J.W., 1995. The 3' untranslated region of picornavirus RNA: features required for efficient genome replication.

85. Romero T.A., Tumban E., Jun J., Lott W.B., Hanley K.A., 2006. Secondary structure of dengue virus type 4 3′-untranslated region: impact of deletion and substitution mutations. J. Gen. Virol 87 (11): 3291–3296.

86. Rosskopf, J.J., Upton III, J.H., Rodarte, L., Romero, T.A., Leung, M., Taufer, M., Johnson, K.L., 2010. A 3' terminal stem-loop structure in Nodamura virus RNA2 forms an essential cis-acting signal for RNA replication. Virus Res. 150, 12-21.

87. Sambrook, J., Russell, D.W., 2001. Molecular cloning: a laboratory manual, third ed. Cold Spring Harbor, NY.

88. Scherer, W.F., Hurlbut, H.S., 1967. Nodamura virus from Japan: a new and unusual arbovirus resistant to diethyl ether and chloroform. Am. J. Epidemiol. 86 (2): 271-285.

89. Selling, B.H., Allison, R.F., Kaesberg, P, 1990. Genomic RNA of an insect virus directs synthesis of infectious virions in plants. PNAS 87 (1): 434-438.

90. Shi, P.-Y., Brinton, M.A., Veal, J.M., Zhong, Y.Y., Wilson, W.D., 1996. Evidence for the existence of a pseudoknot structure at the 3' terminus of the flavivirus genomic RNA.

91. Sit, T.L., Vaewhongs, A.A., Lommel, S.A., 1998. RNA-mediated trans-activation of transcription from a viral RNA. Science 281: 829-832.

92. Studnicka, G.M., Rahn, G.M., Cummings, I.W., Salser, W.A., 1978. Computer method for predicting the secondary structure of single-stranded RNA. Nucl. Acids. Res. 5 (9): 3365-3387.

93. Sullivan, C.S., Ganem, D., 2005. A virus-encoded inhibitor that blocks RNA interference in mammalian cells. J. Virol. 79 (12): 7371-7379.

94. Sztuba-Solińska, J., Stollar, V., Bujarski, J.J. 2011. Subgenomic messenger RNAs: mastering regulation of (+)-strand RNA virus life cycle. Virol. 412 (2): 245-255.

95. Tan, Z., Chen, S., 2011. Salt contribution to RNA tertiary structure folding stability. Biophys J. 101 (1): 176-187.

96. Taufer, M., Leung, M., Solorio, T., Licon, A., Mireles, D., Araiza, R., Johnson, K.L., 2008. RNAVLab: a virtual laboratory for studying RNA secondary structures based on grid computing technology. Parallel Computing 34: 661-680.

97. ten Dam, E., Pleij, K., Draper, D., 1992. Structural and functional aspects of RNA pseudoknots. Persp. In Biochem. 31 (47): 11665-11676.

98. Thiery, R., Johnson, K.L., Nakai, T., Schneemann, A., Bonami, J.-R., Lightner, D.V., 2011. Family Nodaviridae, in: King, A.M.Q., Adams, M.J., Carstens, E.B., Lefkowitz, E.J. (Eds.), Virus Taxonomy. Ninth Report of the International Committee on Taxonomy of Viruses. Elsevier Academic Press, Waltham, MA, pp. 1061-1067.

99. Thomas, P.S., 1980. Hybridization of denatured RNA and small DNA fragments transferred to nitrocellulose. PNAS 77 (9): 5201-5205.

100. Tilgner, M., Shi, P.-Y., 2004. Structure and function of the 3' terminal six nucleotides of the *West Nile Virus* genome in viral replication. J. Virol. 78 (15): 8159-8171.

101. Tinoco Jr., I., Uhlenbeck, O.C., Levine, M.D, 1971. Estimation of secondary structure in ribonucleic acids. Nature 230: 362-366.

102. Tinoco Jr., I., Bustamante, C., 1999. How RNA folds. J. Mol. Biol. 293 (2): 271-281.

103. Tukey, J.W., 1977. Exploratory Data Analysis, first ed. Addison-Wesley.

104. Tuplin, A., Evans, D.J., Simmonds, P., 2004. Detailed mapping of RNA secondary structures in core and NS5B-encoding region sequences of hepatitis C virus by RNase cleavage and novel bioinformatic prediction methods. J. Gen. Virol 85: 3037-3047.

105. Van Wynsberghe, P.M., Ahlquist, P., 2009. 5' cis elements direct nodavirus RNA1 recruitment to mitochondrial sites of replication complex formation J. Virol. 83 (7): 2976-2988.

106. Waugh, A., Gendron, P., Altman, R., Brown, J.W., Case, D., Gautheret, D., Harvey, S.C., Leontis, N., Westbrook, J., Westhof, E., Zuker, M., Major, F., 2002. RNAML: a standard synthax for exchanging RNA information. RNA 8 (6): 707-717.

107. Westhoff, E., Jaeger, L., 1992. RNA pseudoknots. Curr. Opin. In Struc. Biol. 2: 327-333.

108. White, K.A., 2002. The premature termination model: a possible third method for subgenomic mRNA transcription in (+)-strand RNA viruses. 304 (2): 147-154.

109. Williams, G.D., Chang, R.-Y., Brian, D.A., 1999. A phylogenetically conserved hairpin-type 3' untranslated region pseudoknot functions in coronavirus RNA replication.

110. Wyatt, J.R., Puglisi, J.D., Tinoco Jr., I., 1990. RNA pseudoknots: stability and loop size requirements. J. Mol. Biol. 214: 455-470.

111. Yot, P., Pinck, M., Haenni, A.L., Duranton, H.M., Chapeville, F. 1970. Proc. Nat. Acad. Sci. 67: 1345-1352.

112. Zeddam, JL., Rodrigues, J.L., Ravallec, M., Lagnaoui, A., 1999. A noda-like virus isolated from the sweetpotato pest *Spodoptera eridania* (Cramer) (Lep; *Noctuidae*). J. Invert. Path. 74 (3): 267-274.

113. Zhong, W., Dasgupta, R., Rueckert, R., 1992. Evidence that the packaging signal for nodaviral RNA2 is a bulged stem-loop. PNAS 89 (23): 11146-11150.

114. Zhong, W., Rueckert, R.R., 1993. Flock house virus: down-regulation of subgenomic RNA3 synthesis does not involve coat protein and is targeted to synthesis of its positive strand. J. Virol. 67 (5): 2716-2722.

115. Zuker, M., 2003. Mfold web server for nucleic acid folding and hybridization prediction. Nucleic Acids Res. 31 (13): 3406-3415.

116 Zuker, M., Jacobson A.B., 1998. Using Reliability Information to Annotate RNA Secondary Structures. RNA 4: 669-679.

117. Zuker, M., Stiegler, P., 1981. Optimal computer folding of large RNA sequences using thermodynamics and auxiliary information. Nucl. Acids Res. 9 (1): 133-148.

CURRICULUM VITA

Joshua P. Frederick was born in New Orleans, LA., 1988, to parents Lee. H. Frederick and Janet G. Frederick. He grew up in Orlando, FL and El Paso, TX, where he graduated from Franklin High School in 2006. He earned his Bachelor's of Science in Biology with a minor in Secondary Education at the University of Texas at El Paso (UTEP) in the winter of 2009. During his studies, Josh received Science 8-12 certification from the Texas State Board of Educator Certification. In the fall of 2010, Josh entered the Master's of Science program under the Biological Sciences Department at UTEP. While studying, Josh was fortunate enough to attend and present at the 30th Annual Meeting of the American Society for Virology in Minneapolis, MN, where he received a Student Travel Award. Josh graduated with his Master's of Science in Biological Sciences in the winter of 2012.

Permanent residence:

1300 Randolph Dr.
El Paso, TX 79902